HYDROLOGICAL MODELING OF LAKE PREVATT, ORANGE COUNTY, FLORIDA

By:

Shiblu Sarker, Ph.D., P.E.
Awes Karama, Ph.D.
Holli N. Capps Herron
Tom Jobes

St. Johns River Water Management District

Palatka, Florida

2024


Northwest Florida Water Management District
Suwannee River Water Management District
St. Johns River Water Management District
Southwest Florida Water Management District
South Florida Water Management District
ST. JOHNS RIVER WATER MANAGEMENT DISTRICT

TABLE OF CONTENTS

Table of Contents iii
Table of Figures iv
Table of Tables v
Executive Summary 1
Background 2
Existing Data Review 3
  Meteorological Data 3
  Groundwater Level Data 5
  Observed Stage Data 8
  Digital Elevation Model 11
  Watershed Delineation 12
  Other Geospatial Data 13
Model Development 16
  Land Cover and Soils 16
  Water Body Characteristics 17
  Groundwater Losses from Lake to UFA 20
  Variable Lake Surface Area 21
Model Calibration and Validation 22
  Lake Stages 22
  Water Balance 29
Sensitivity Analysis 31
Long-term Simulation 43
Summary and Conclusions 45
References 46
Attachment 47

TABLE OF FIGURES

Figure 1. Lake Prevatt and its watershed 2
Figure 2. NEXRAD pixels and weather station locations for Lake Prevatt 4
Figure 3. Annual rainfall for Isle-Win and NEXRAD, and annual PET for Lisbon 5
Figure 4. Locations of UFA wells 6
Figure 5. Correlation between observed UFA groundwater levels (ft NAVD88) 7
Figure 6. Observed and extended UFA groundwater levels (ft NAVD88) 7
Figure 7. Stage recorders and surficial aquifer well locations 8
Figure 8. Observed North Lobe, South Lobe and surficial aquifer water levels (ft NAVD88) 9
Figure 9. Correlation between South Lobe stage and the surficial aquifer water level (ft NAVD88) 10
Figure 10. Comparison of North Lobe observed data and South Lobe extended data (ft NAVD88) 11
Figure 11. Topobathymetric DEM for Lake Prevatt watershed (ft NAVD88) 12
Figure 12. Subwatershed delineation for North and South Lobes 13
Figure 13. Model land cover categories 14
Figure 14. Soil hydrologic groups of the study area 15
Figure 15. Stage-area and stage-volume relationship for the North Lobe (ft NAVD88) 17
Figure 16. Stage-area and stage-volume relationship for the South Lobe (ft NAVD88) 18
Figure 17: Schematic of ICPR model for lake stage-discharge relationship 19
Figure 18. Lake Prevatt stage-discharge relationship 20
Figure 19. Observed and simulated daily stages for the North Lobe of Lake Prevatt for calibration period (ft NAVD88) 23
Figure 20. Observed and simulated daily exceedance probability curves for North Lobe for calibration period (ft NAVD88) 24
Figure 21. Observed/extended and simulated daily stages for the South Lobe of Lake Prevatt for calibration period (ft NAVD88) 25
Figure 22. Observed and simulated daily exceedance probability curves for South Lobe for calibration period (ft NAVD88) 26
Figure 23. Observed and simulated daily stages for the North Lobe of Lake Prevatt for validation period (ft NAVD88) 27
Figure 24. Observed and simulated daily exceedance probability curves for North Lobe for validation period (ft NAVD88) 28
Figure 25. Impact of leakance value on simulated stages of the North Lobe of Lake Prevatt (ft NAVD88) 33
Figure 26. Impact of leakance value on simulated stages of the South Lobe of Lake Prevatt (ft NAVD88) 34
Figure 27. Impact of LZSN on simulated stages of the North Lobe of Lake Prevatt (ft NAVD88) 35
Figure 28. Impact of LZSN on simulated stages of the South Lobe of Lake Prevatt (ft NAVD88) 36
Figure 29. Impact of DEEPFR on simulated stages of the North Lobe of Lake Prevatt (ft NAVD88) 37
Figure 30. Impact of DEEPFR on simulated stages of the South Lobe of Lake Prevatt (ft NAVD88) 38
Figure 31. Impact of LZETP on simulated stages of the North Lobe of Lake Prevatt (ft NAVD88) 39

Figure 32. Impact of LZETP on simulated stages of the South Lobe of Lake Prevatt (ft NAVD88) 40
Figure 33. Impact of INFILT on simulated stages of the North Lobe of Lake Prevatt (ft NAVD88) 41
Figure 34. Impact of INFILT on simulated stages of the South Lobe of Lake Prevatt (ft NAVD88) 42
Figure 35. Daily long-term observed and simulated stages of the North Lobe of Lake Prevatt (ft NAVD88) 43
Figure 36. Daily long-term observed and simulated stages of the South Lobe of Lake Prevatt (ft NAVD88) 44

TABLE OF TABLES

Table 1. Summary of Rainfall and PET time series data 5
Table 2. Land cover areas within the Lake Prevatt watershed 16
Table 3. Hydrologic soil group areas within the Lake Prevatt watershed 16
Table 4. Calibrated values for principal hydrology parameters. 22
Table 5. Goodness-of-fit statistics for daily North Lobe stages simulation 28
Table 6. Goodness-of-fit statistics for daily South Lobe stages simulation 29
Table 7. Annual average water budget for the calibration period per land-use in inches per year 29
Table 8. Annual average water budget for the validation period per land-use in inches per year 29
Table 9. Annual average water budget for North Lobe in acre-feet 30
Table 10. Annual average water budget for South Lobe in acre-feet 30
Table 11. Impact on model goodness-of-fit statistics compared to calibrated values for North Lobe 32
Table 12. Impact on model goodness-of-fit statistics compared to calibrated values for South Lobe 32

EXECUTIVE SUMMARY

The St. Johns River Water Management District (SJRWMD) has been working to establish Minimum Flows and Levels (MFLs) for Lake Prevatt. The MFL program designates the minimum hydrologic conditions that must be maintained for the lake to prevent significant harm to water resources and ecosystem services resulting from permitted water withdrawals. In support of the MFLs program, SJRWMD developed a Hydrological Simulation Program - FORTRAN (HSPF) model to simulate the hydrologic and hydraulic processes, surface water – groundwater interaction, and water budget components of Lake Prevatt and its watershed.

Using the existing available hydro-meteorological and geospatial data, the HSPF model was set up for the period from 1995 to 2020. The model was calibrated and validated for the periods 2008 to 2020 and 1995 to 2007, respectively. Model performance was evaluated with common graphical methods and statistical metrics used by SJRWMD. Once successfully calibrated and validated, the model was extended to the period from 1953 to 2020 for long-term simulations.

The HSPF model reasonably simulated the temporal variations and magnitudes of observed stages for Lake Prevatt during both the calibration and validation periods. Most importantly, the model adequately replicated the observed low to medium stages of Lake Prevatt, which are crucial for MFLs modeling and assessment processes. Some discrepancies between the long-term observed and simulated stages are noticed; however, this decrease in performance in the earlier years could be attributed to the lack of long-term observed groundwater and rainfall data within the watershed, as well as land use/land cover changes in the watershed due to urban development, as were apparent in a comparison of historic aerial photos. Sensitivity analysis found that the lakebed leakance and the lower zone evapotranspiration parameter are the most sensitive parameters for the model. Overall, the HSPF model showed reasonable simulations of hydrologic and surface water - groundwater interaction processes of the lake. Therefore, it is concluded that the model can be used for MFLs modeling and scenarios analysis.

BACKGROUND

The St. Johns River Water Management District (SJRWMD) has been working to establish Minimum Flows and Levels (MFLs) for Lake Prevatt. The MFL program designates the minimum hydrologic conditions that must be maintained for the lake to prevent significant harm to water resources and ecosystem services resulting from permitted water withdrawals. In support of the MFLs program, SJRWMD developed a Hydrological Simulation Program - FORTRAN (HSPF) model to simulate the hydrologic and hydraulic processes, surface water – groundwater interaction, and water budget components of Lake Prevatt and its watershed.

Lake Prevatt is located in the Wekiva River Watershed, within Orange County, Florida. It lies two miles north of the City of Apopka in Wekiwa Springs State Park. It has a surface area of approximately 100 acres, and discharges via Carpenter Branch and Mills Creek into Rock Springs Run. The location of the lake and its watershed are shown in Figure 1Figure 1. At low stages, the lake separates into two lobes, called the North Lobe and the South Lobe.

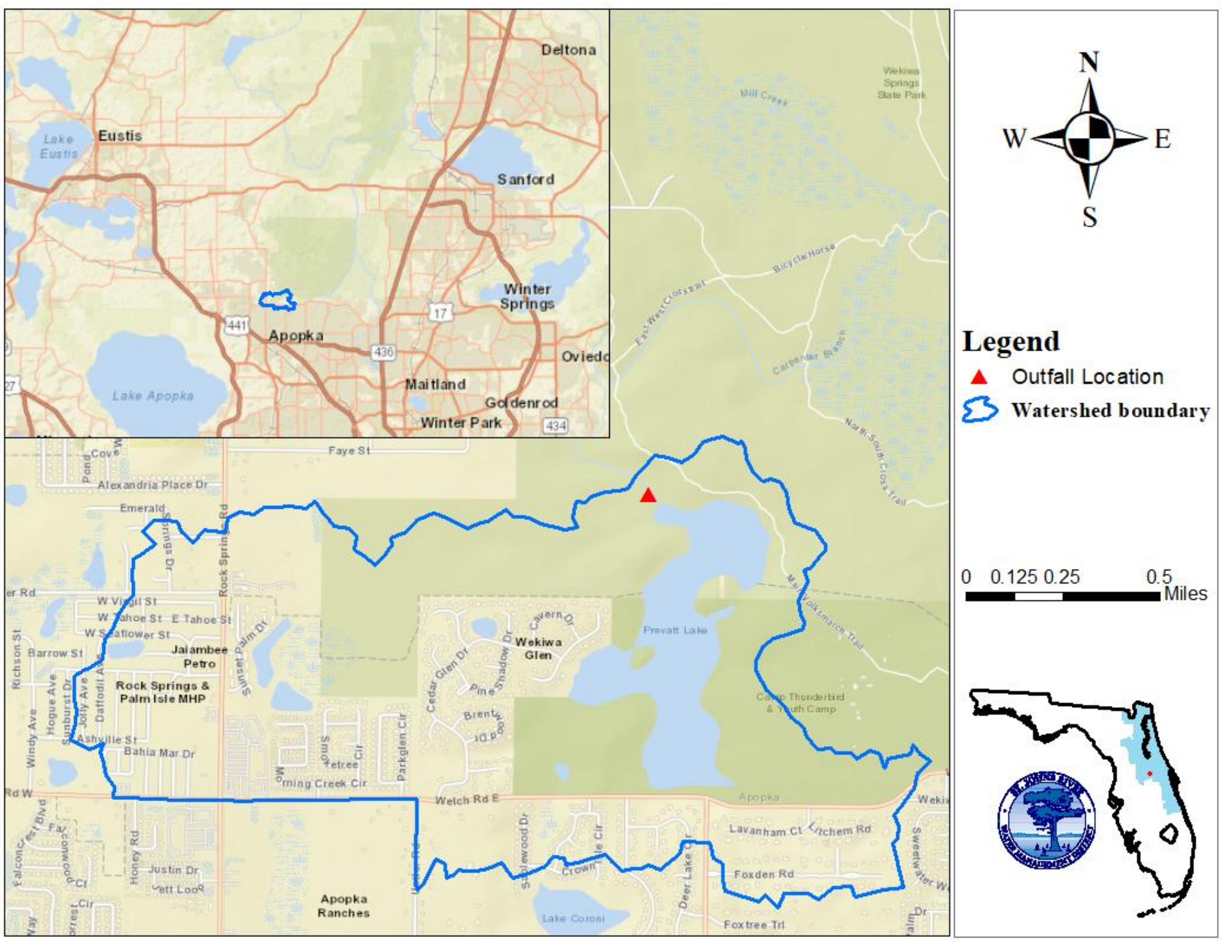

Figure 1. Lake Prevatt and its watershed

EXISTING DATA REVIEW

SJRWMD obtained and reviewed the following available data to set up the HSPF model for the Lake Prevatt watershed:

- Rainfall and potential evapotranspiration (PET) data
- Observed groundwater levels
- Observed lake levels
- Geospatial data such as digital elevation model (DEM), lake bathymetry, land use/land cover (LULC), and soils

Meteorological Data

SJRWMD reviewed several meteorological stations and Next Generation Weather Radar (NEXRAD) pixels for rainfall data. Figure 2 shows the station locations from this review. The area-weighted average of NEXRAD data was determined to be the most accurate source for rainfall within the Lake Prevatt watershed. Therefore, we have used this as the source of rainfall data for the model calibration. However, the long-term simulation required available data dating back to the early 1950s, but NEXRAD records only begin in 1995. Therefore Isle-Win, the closest rainfall station, was used to extend the long-term rainfall record back to 1953. The closest available PET station was Lisbon, which was used for both the calibration and long-term simulation models. Figure 3 shows annual totals for the meteorological data used, and summary statistics for each source is shown in Table 1.

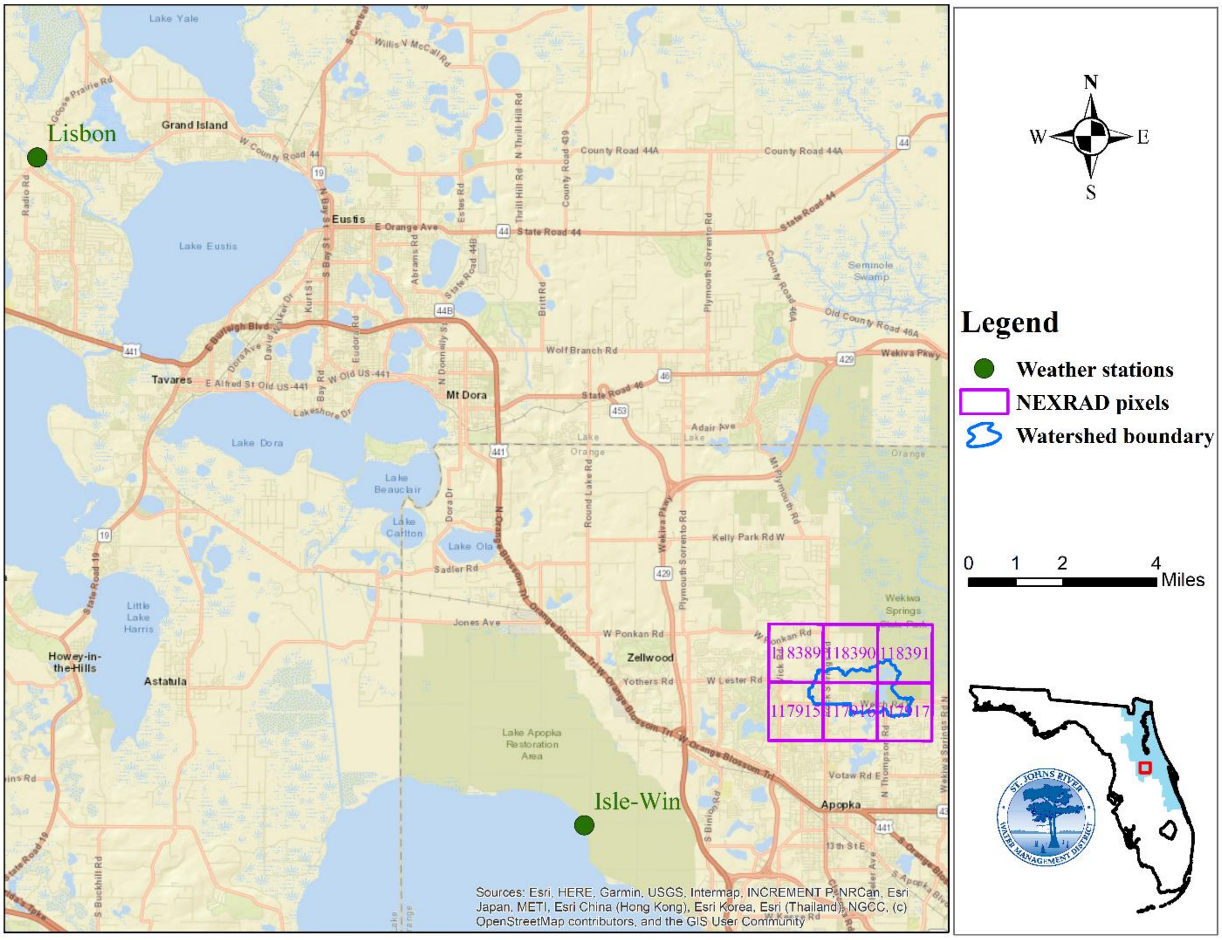

Figure 2. NEXRAD pixels and weather station locations for Lake Prevatt

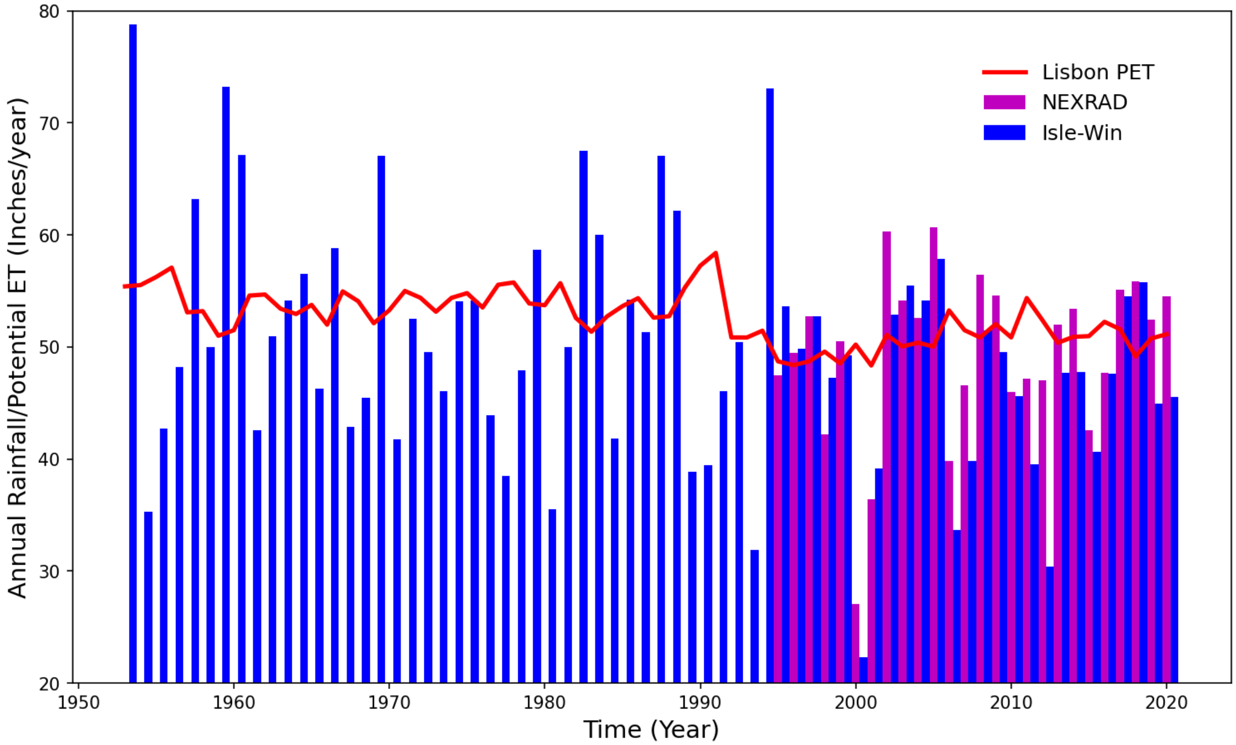

Figure 3. Annual rainfall for Isle-Win and NEXRAD, and annual PET for Lisbon

Table 1. Summary of Rainfall and PET time series data

	NEXRAD	**Isle-Win**	**Lisbon PET**
Minimum (inches/year)	27.04	22.28	48.34
Maximum (inches/year)	60.63	78.78	58.39
Mean (inches/year)	49.41	49.83	52.63
Start date	1995-01-03	1953-01-01	1953-01-01
End date	2020-12-31	2020-12-31	2020-12-31

Groundwater Level Data

Groundwater level data is needed to set a boundary condition for the loss of water from the lake to the Upper Floridan Aquifer (UFA). The suitability of three nearby UFA wells was evaluated. Figure 4 shows their locations. Well OR0893 is located inside the watershed and therefore was used for its available period of record, from 1/1/2009 to 12/30/2020. For extending the record back further, the Line of Organic Correlation method (LOC) (Helsel & Hirsch, 2002) was used to determine correlations between this well and the other two more distant ones. The record for the next closest well OR0548 went back to 11/19/1992. For the long-term simulation, it was necessary to use the furthest well S-0125.

OR0548 had a good correlation with OR0893, with a coefficient of determination (R^2) of 0.70. S-0125 had a reasonable correlation with OR0893, with an R^2 of 0.48. Figure 5 shows scatter plots, LOC equations, and R^2 values for each secondary well. Figure 6 shows the UFA groundwater levels for the individual wells and the final extended data set. Note that all elevation data in this report, whether groundwater (GW) levels, lake levels, or topography, are in feet above the North American Vertical Datum (NAVD), 1988.

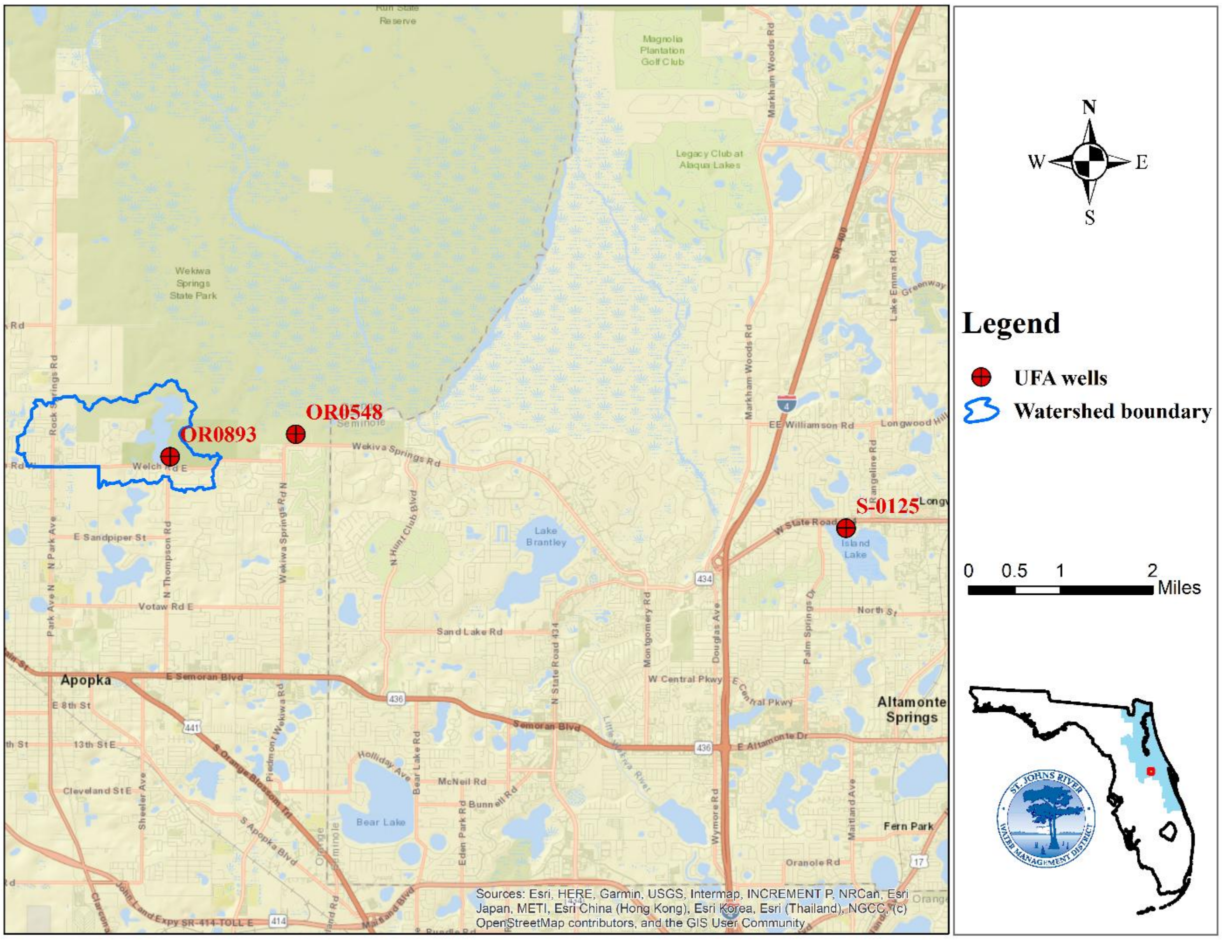

Figure 4. Locations of UFA wells

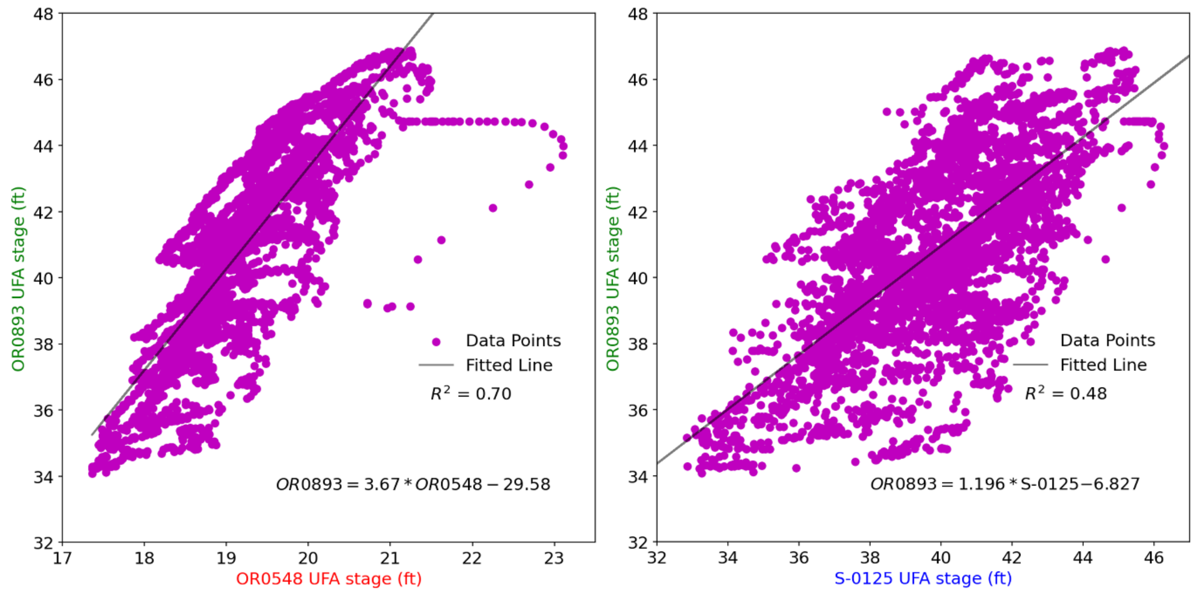

Figure 5. Correlation between observed UFA groundwater levels (ft NAVD88)

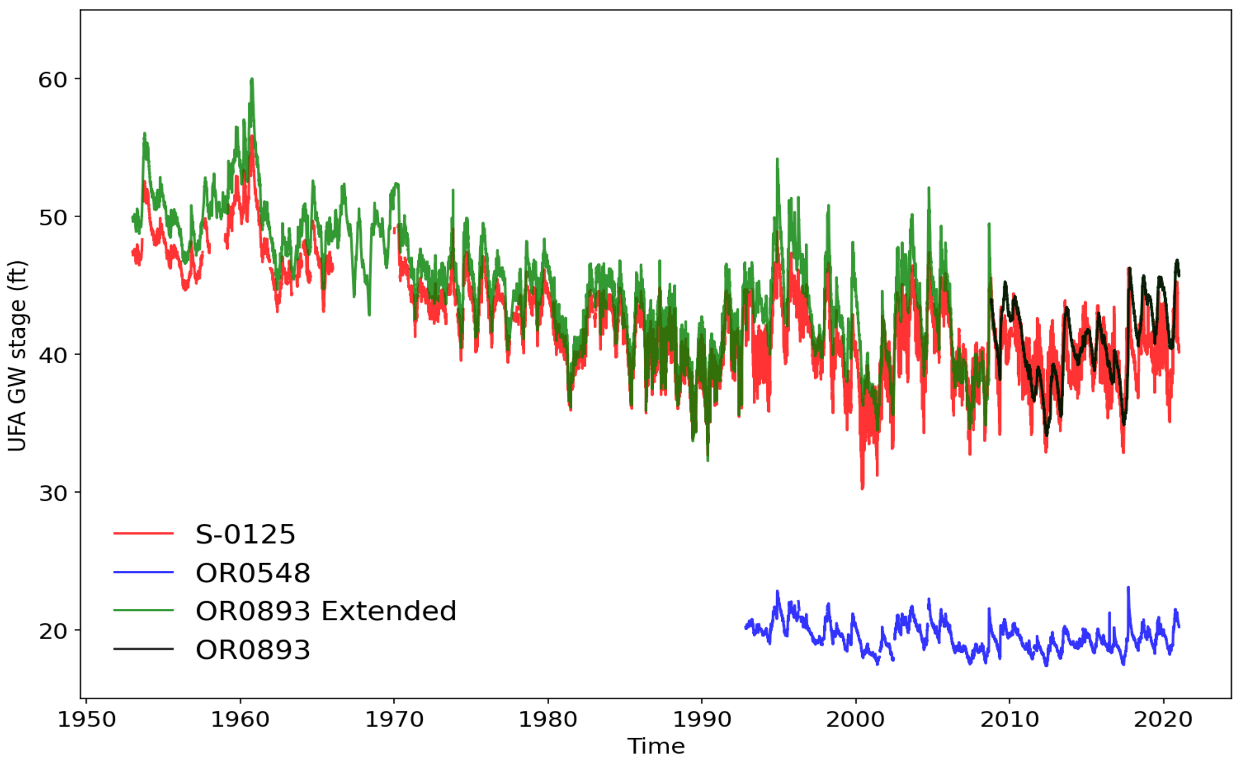

Figure 6. Observed and extended UFA groundwater levels (ft NAVD88)

Observed Stage Data

There is an existing stage recorder with a good record on the north shore of Lake Prevatt (SJRWMD 15470818). However, at low stage the lake divides into two separate North and South Lobes, potentially with different stages. Therefore, an additional station (SJRWMD 15472917) was added to collect stage data in the South Lobe in 2022. Because its record is so short, it was extended by using the LOC method to develop a relationship between it and the data from a nearby surficial aquifer well (OR0894). The locations of the stage recorders and the surficial aquifer well are shown in Figure 7, and the water level records are shown in Figure 8.

Figure 9 shows the scatter plot, and R^2 value for the stage in the South Lobe versus the well water levels. A near perfect correlation ($R^2 = 0.99$) was observed between the surficial aquifer and South Lobe. This is expected since the well is very close to the South Lobe data collection location. The resulting LOC equation used for extension is also shown.

The resulting extended South Lobe timeseries was generally lower than the North Lobe data, even at North Lobe stages above 51 ft, where the two should be connected. The difference in stage was generally about 1 foot. Therefore, we further adjusted the overall extended South Lobe data upward by 1 ft. The North Lobe stage and the extension of the South Lobe stage, before and after adjustment, are shown in Figure 10.

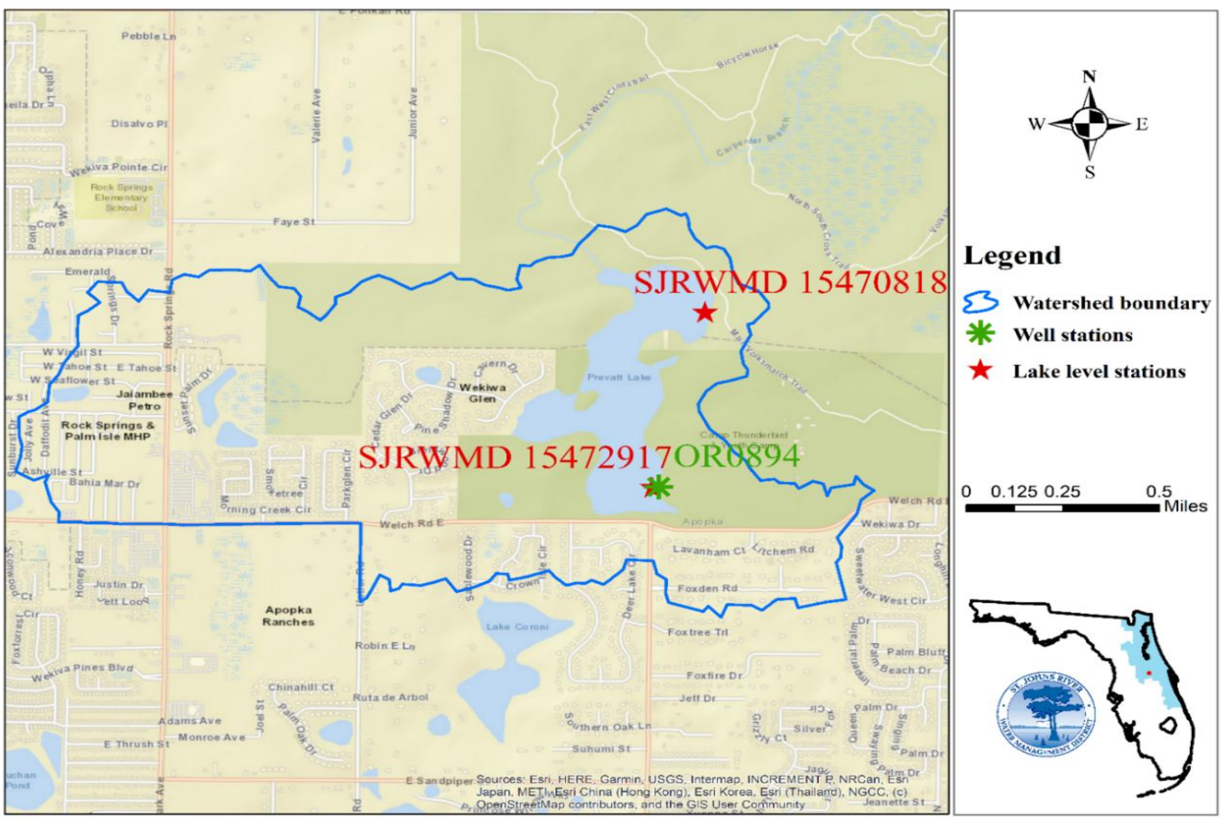

Figure 7. Stage recorders and surficial aquifer well locations

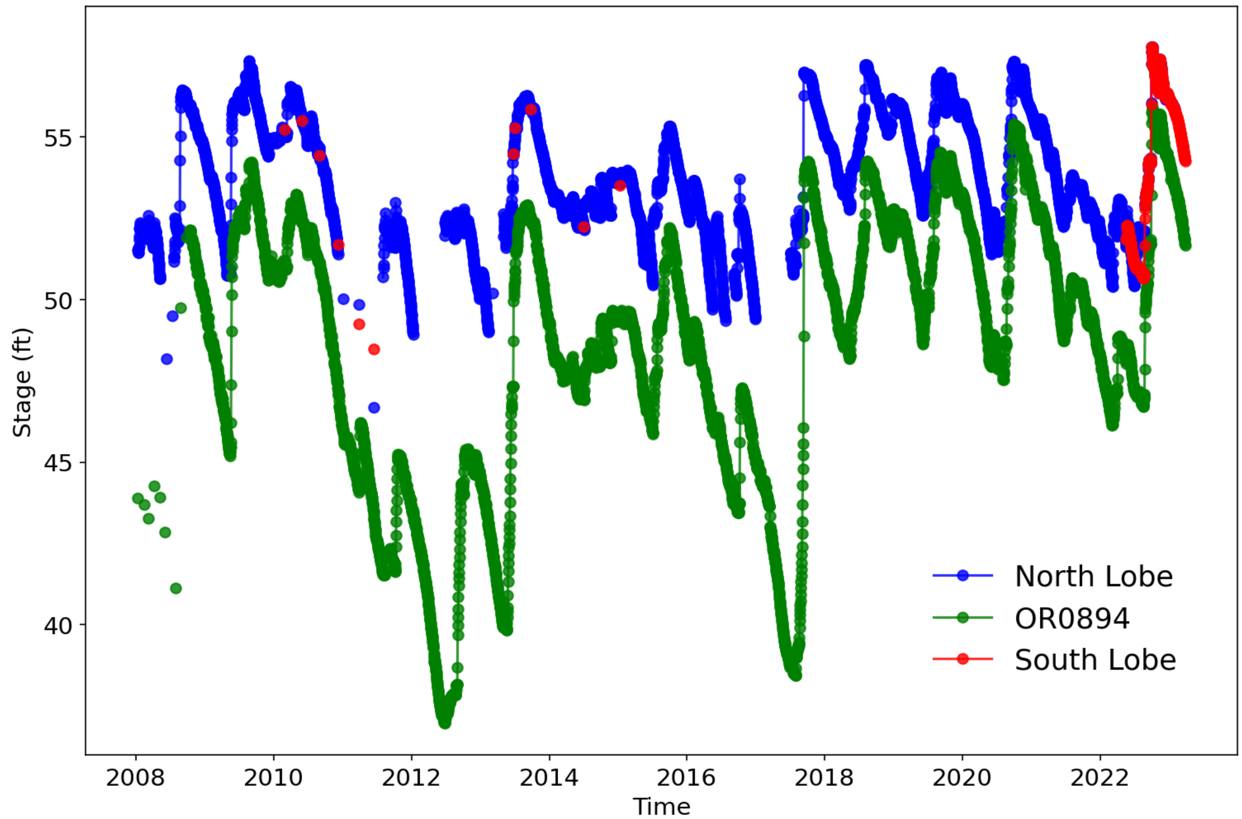

Figure 8. Observed North Lobe, South Lobe and surficial aquifer water levels (ft NAVD88)

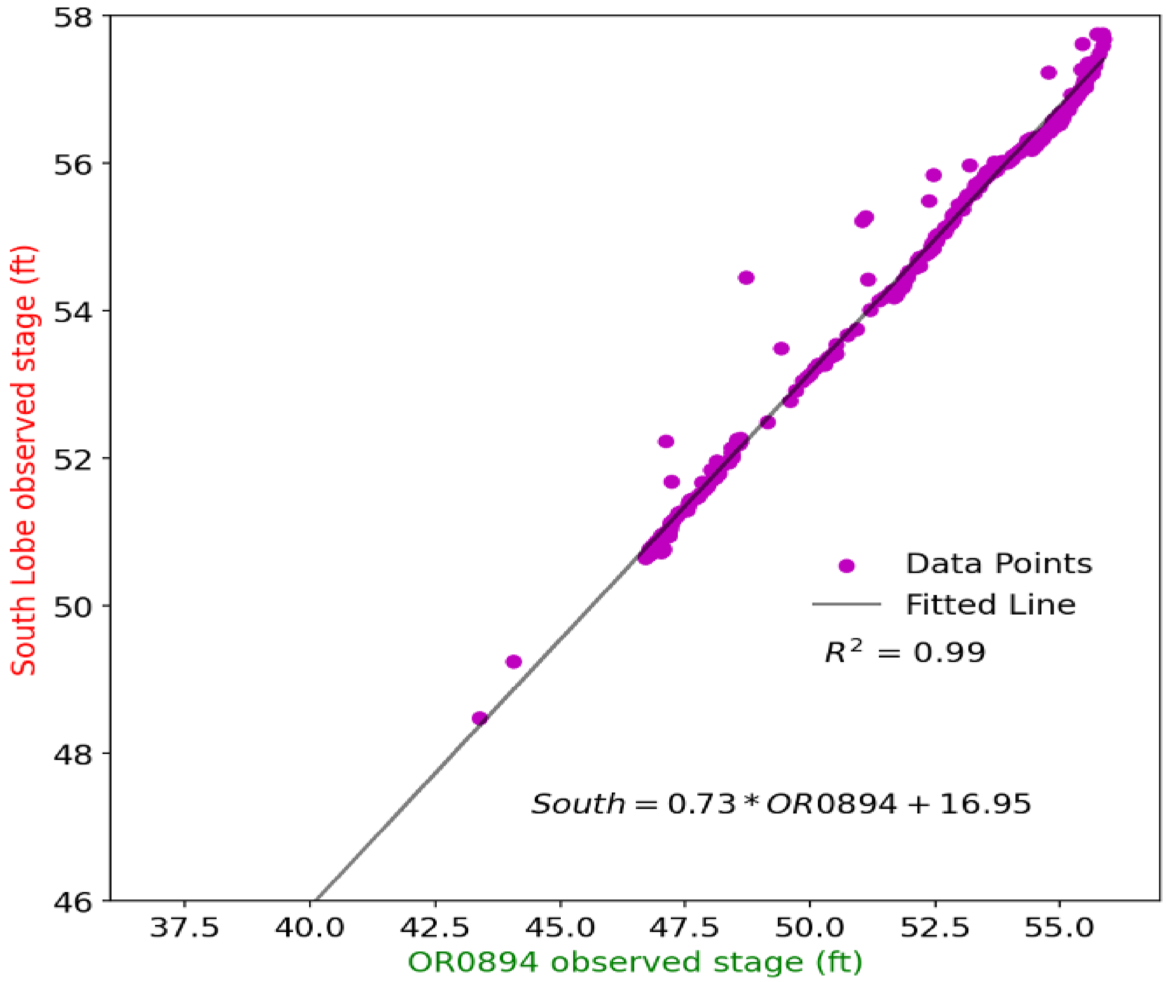

Figure 9. Correlation between South Lobe stage and the surficial aquifer water level (ft NAVD88)

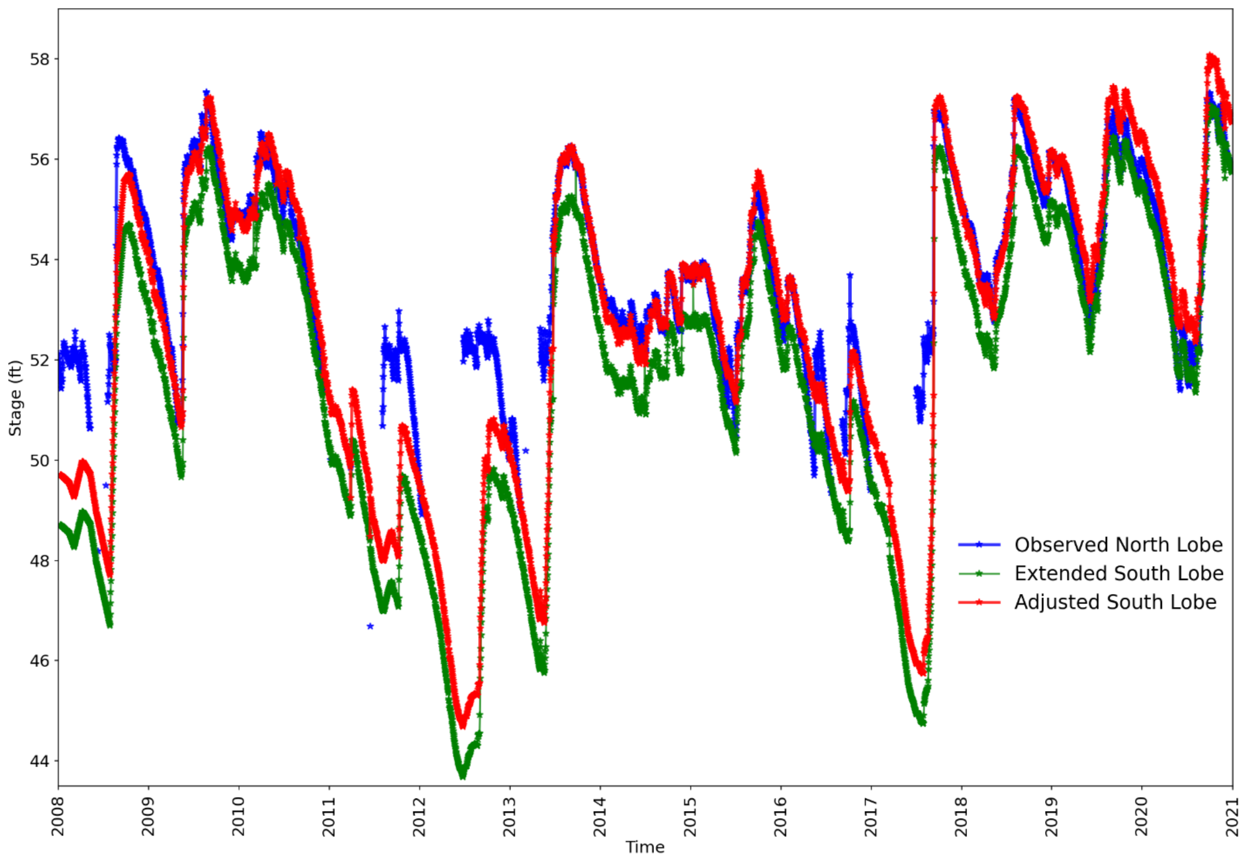

Figure 10. Comparison of North Lobe observed data and South Lobe extended data (ft NAVD88)

Digital Elevation Model

SJRWMD created a Digital Elevation Model (DEM) of the watershed. This process began with the 2018 USGS statewide Light Detection and Ranging (LiDAR)-based DEM collection. Adjustments were then made based on survey data to account for wetland vegetation, which can cause artificially high LiDAR values (Fox, 2023).

Available bathymetry data included acoustic Doppler data from 2015 and manual surveys from 2016, 2021, and 2022. The lake edge was defined by a combination of these data and manual digitization of the lake boundary from aerial photography taken in 1984 and 2014-2017. From these sources, a bathymetric DEM was created. This was then merged with the watershed DEM to generate the final topobathymetric data used for this study, shown in Figure 11. The boundary between the watershed DEM and the bathymetry DEM is also shown.

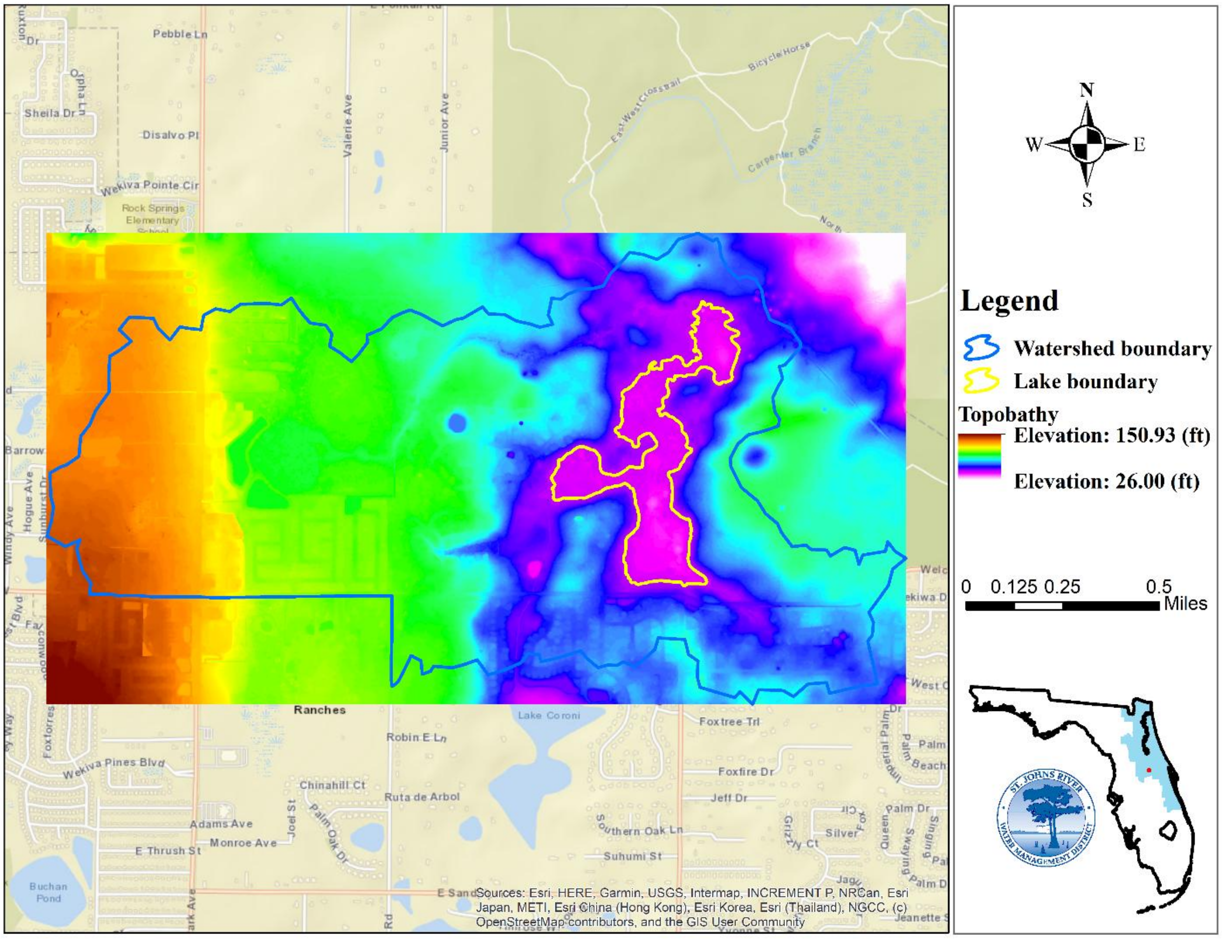

Figure 11. Topobathymetric DEM for Lake Prevatt watershed (ft NAVD88)

Watershed Delineation

The Lake Prevatt watershed was divided into two distinct subwatersheds, shown in Figure 12, to provide separate runoff volumes to the North and South Lobes of the lake. The delineation of Lake Prevatt's subwatersheds was done based on the topobathymetric data using standard ArcGIS Spatial Analyst hydrology tools. The site visits were done to verify the watershed boundary as well as the lake's natural discharge point. The lake connectivity of the two lobes at high stage (above 51 ft) was confirmed with the new bathymetry data as well.

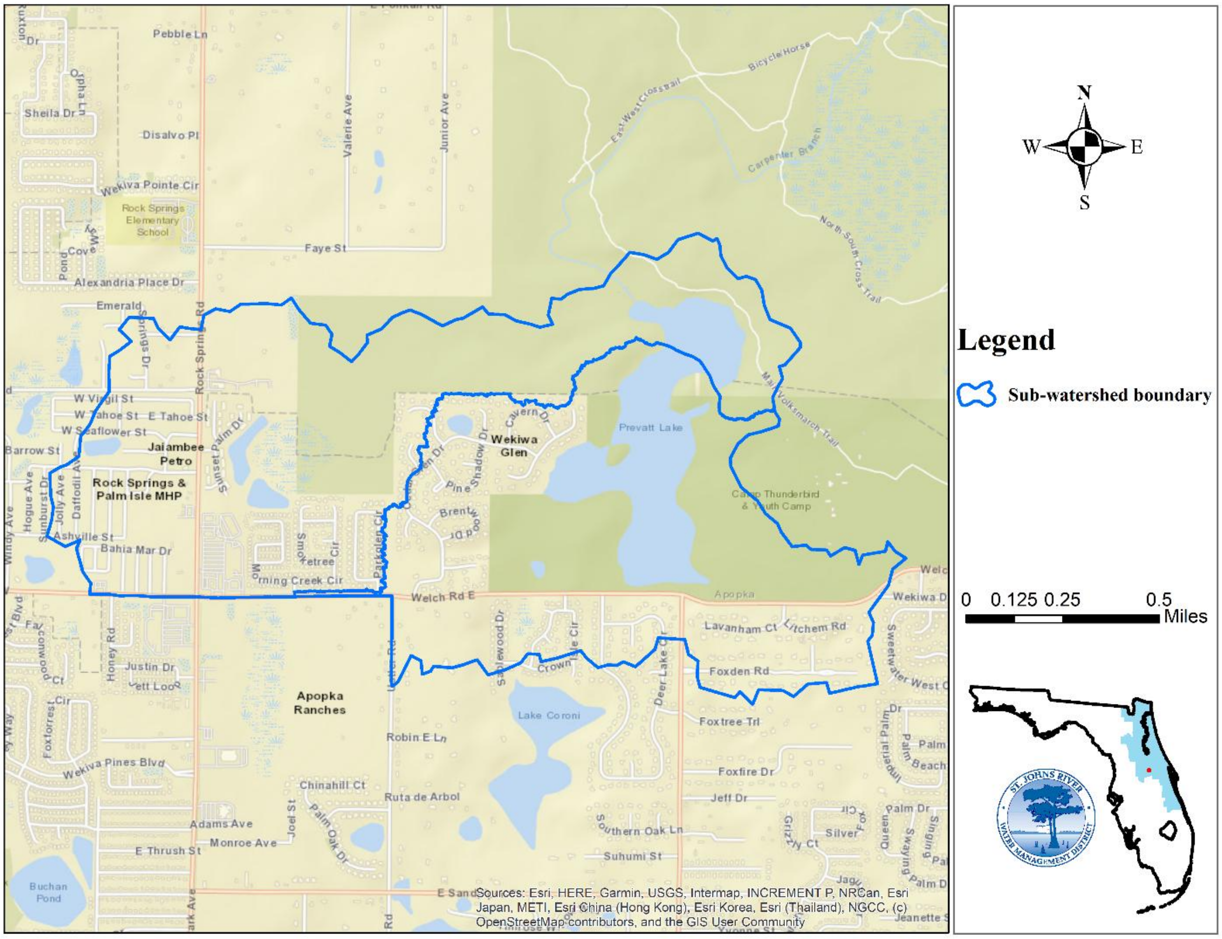

Figure 12. Subwatershed delineation for North and South Lobes

Other Geospatial Data

The 2014 SJRWMD land use and land cover data set was used in this study. The original Florida Land Use Classification Code System (FLUCCS) land cover classes were regrouped into 13 classes following the HSPF land cover grouping method developed for the St Johns River Water Supply Impact Study (Cera et. al., 2012), based mainly on similarities of their hydrologic properties. Figure 13 is a map of the aggregated model land cover categories. The abbreviations for these categories used in this report are: LDR = low density residential; MDR = medium density residential; HDR = high density residential; CI = commercial-industrial; OPN = open land; AGR = agriculture; RNG = rangeland; FRS = forest; WAT=Water; WTL = wetland.

The soil maps were obtained from the Natural Resources Conservation Service (NRCS) Soil Survey Geographic (SSURGO) database. SSURGO classifies soils according to hydrologic groups, shown in Figure 14. The soils in the study area are predominantly type A, which generally consists of well-drained sandy soils. The next most common soil type is A/D, which is well drained when dry but poorly drained when the water table is near the surface.

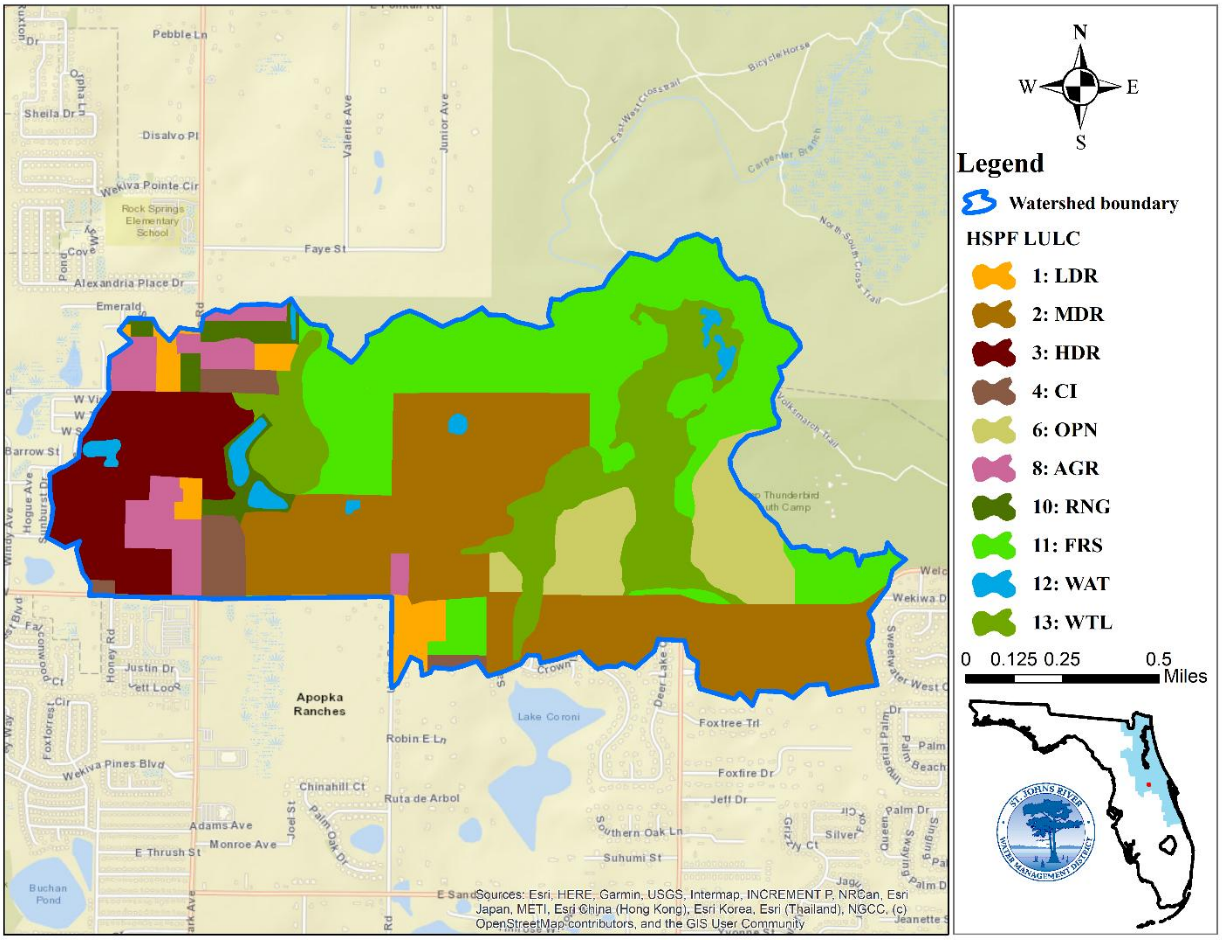

Figure 13. Model land cover categories

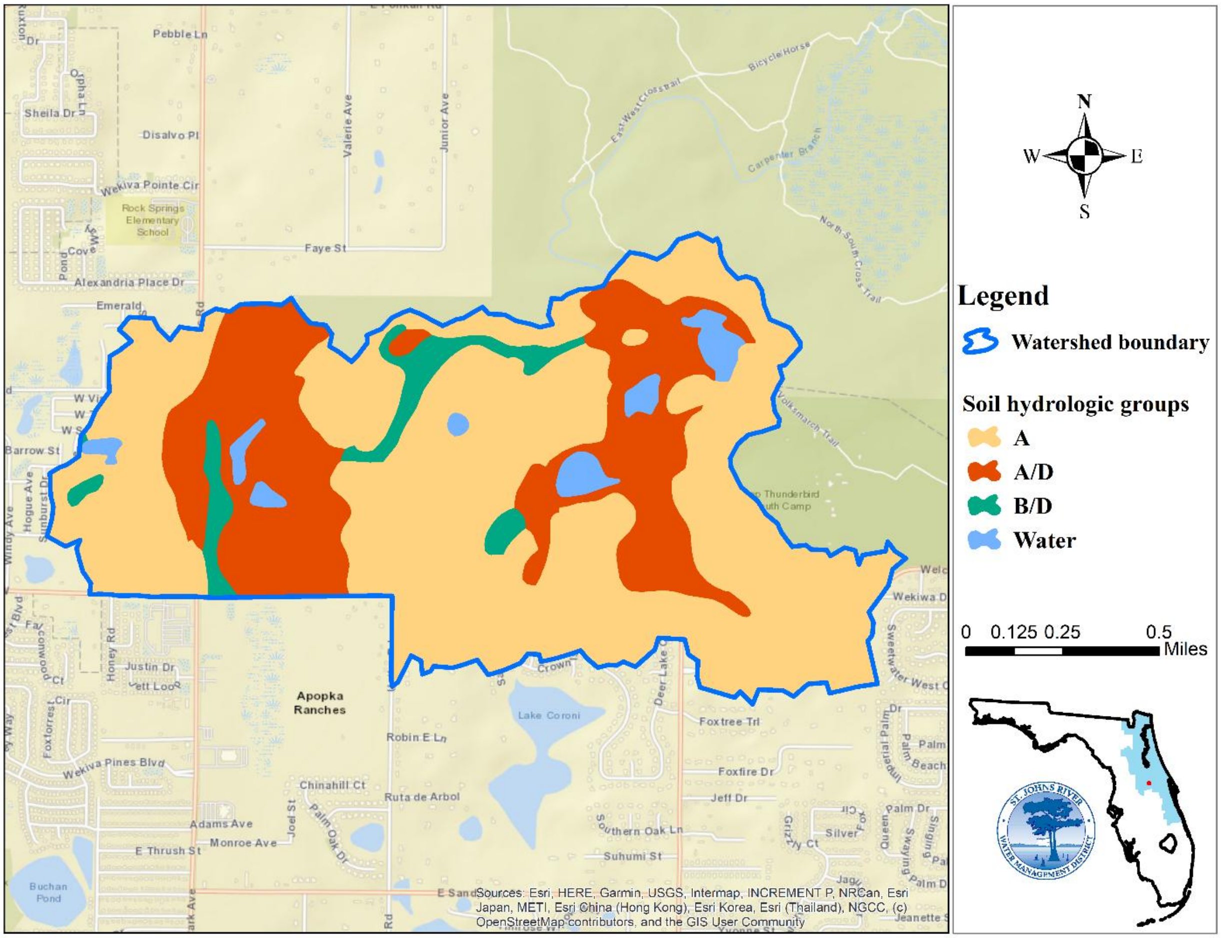

Figure 14. Soil hydrologic groups of the study area

MODEL DEVELOPMENT

The HSPF model was constructed using the hydro-meteorological and geospatial data discussed above for the period 1995 to 2020. Acreages for model land cover and hydrologic soil groups for each subwatershed were computed. Stage/area and stage/volume relationships were developed for the North Lobe and South Lobe based on the topobathymetric DEM. A threshold stage level of 51 ft NAVD was set for the division between the two lobes and the model reaches were set up in such a way that the two lobes effectively become one lake at stages above that level. Also, seepage loss from the lake to the UFA was implemented in the model.

Land Cover and Soils

The land cover data was computed for each subwatershed, summarized in Table 2. Typical impervious fractions of each model land cover category for SJRWMD HSPF models were used. The soil hydrologic group distribution in acreage per subwatershed is summarized in Table 3.

Table 2. Land cover areas within the Lake Prevatt watershed

Land cover	Pervious Area (ac) within North Lobe	Pervious Area (ac) within South Lobe	Impervious Area (ac) within North Lobe	Impervious Area (ac) within South Lobe	Impervious Percentage
1: Low density residential	15.0	14.5	0.8	0.8	5%
2: Medium density residential	62.5	191.6	11.1	33.9	15%
3: High density residential	62.2	0.0	33.5	0.0	35%
4: Commercial/Industrial	12.7	1.5	12.7	1.5	50%
6: Open	0.0	81.7	0.0	0.0	-
8: General agriculture	45.8	3.3	0.0	0.0	-
10: Range	23.3	0.0	0.0	0.0	-
11: Forest	187.5	75.9	0.0	0.0	-
12: Water	15.7	1.5	0.0	0.0	-
13: Wetland	48.3	101.3	0.0	0.0	-

Table 3. Hydrologic soil group areas within the Lake Prevatt watershed

Soil Group	Area (ac) within North Lobe	Area (ac) within South Lobe	Description
A	288.59	395.62	High infiltration rate
A/D	182.61	92.99	High or very low infiltration rate
B/D	40.57	5.12	Moderate or very low infiltration rate
Water	19.14	14.09	Water

Water Body Characteristics

In HSPF the streams and lakes within a subwatershed are represented as a river reach or reservoir segment called RCHRES. The relationships between stage, surface area, volume, and discharge for a RCHRES are represented by a hydraulic function table called an FTABLE, a piecewise-linear function table. From the lake bathymetry data, a detailed stage-area-volume table (see Attachment) was generated for each lobe of the lake using ArcGIS tools. The resulting stage-area and stage-volume curves for the North Lobe and South Lobe are shown in Figure 15 and Figure 16 respectively.

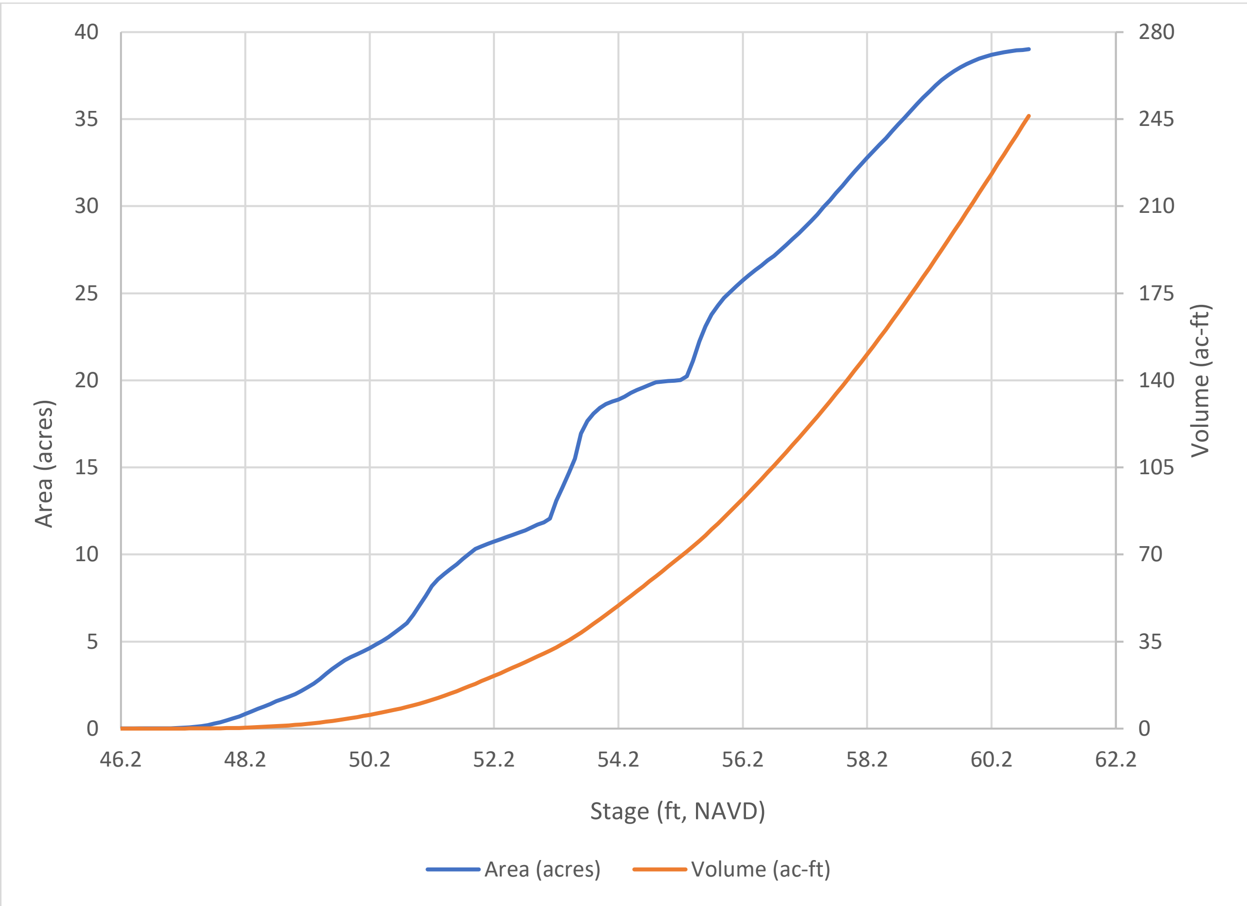

Figure 15. Stage-area and stage-volume relationship for the North Lobe (ft NAVD88)

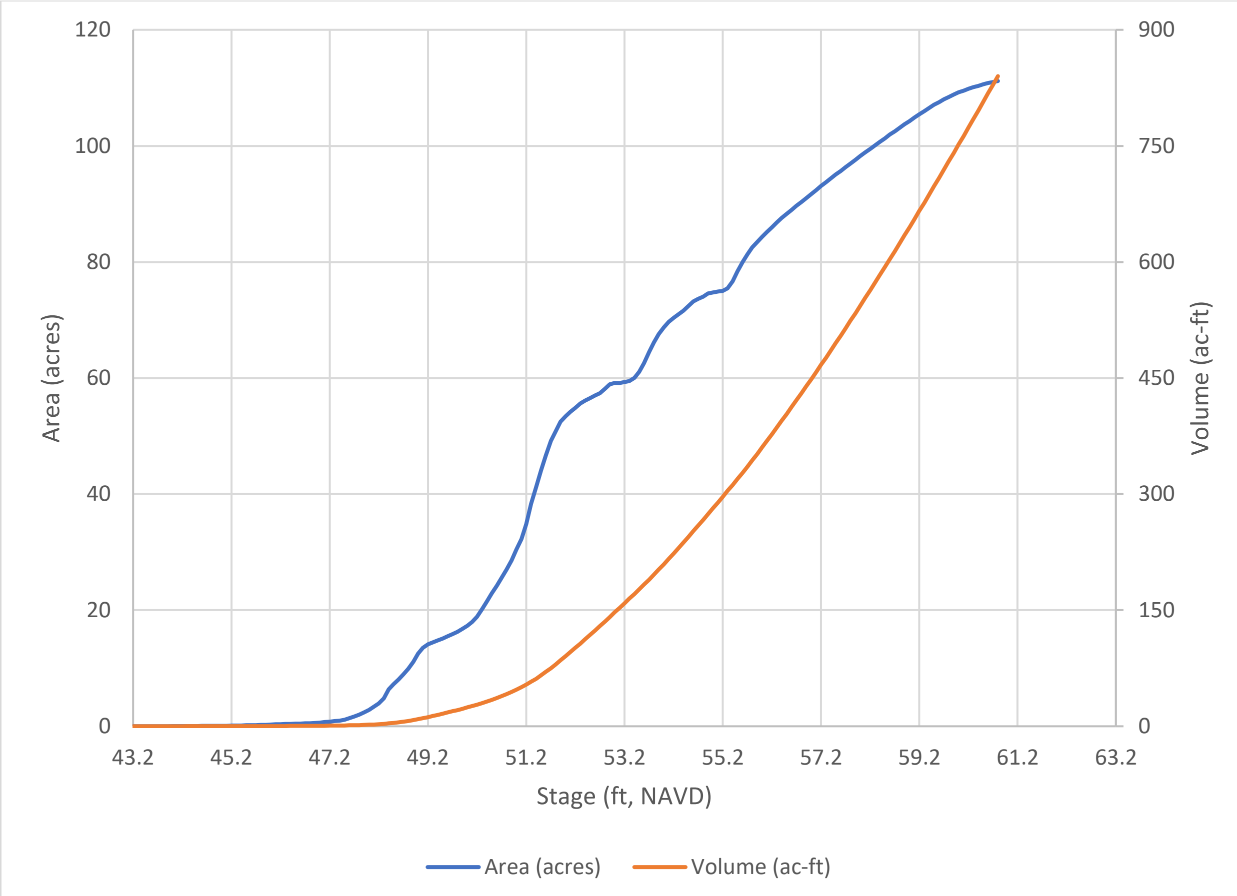

Figure 16. Stage-area and stage-volume relationship for the South Lobe (ft NAVD88)

The stage-flow relationship for the outlet was developed from a simple Interconnected Channel and Pond Routing (ICPR v4) model of the upper part of Carpenter Branch. Cross sections were derived from the topographic DEM with assumed simple channel morphology. Figure 17 shows the model schematic with the approximate geographic locations of the links, nodes, and cross sections. The downstream boundary of this model is at a pair of 36” culverts at a small dirt road crossing, which is represented as a constant head of 44.0 ft NAVD. This crossing is sufficiently lower than the lake invert that a time-varying representation of the tailwater is not necessary for accurate results. The resulting stage-discharge relationship at the lake outlet is shown in Figure 18. The connection between the two lobes is modeled using HSPF Special Actions which balance the stages between lobes when above the saddle point of 51.0 ft NAVD.

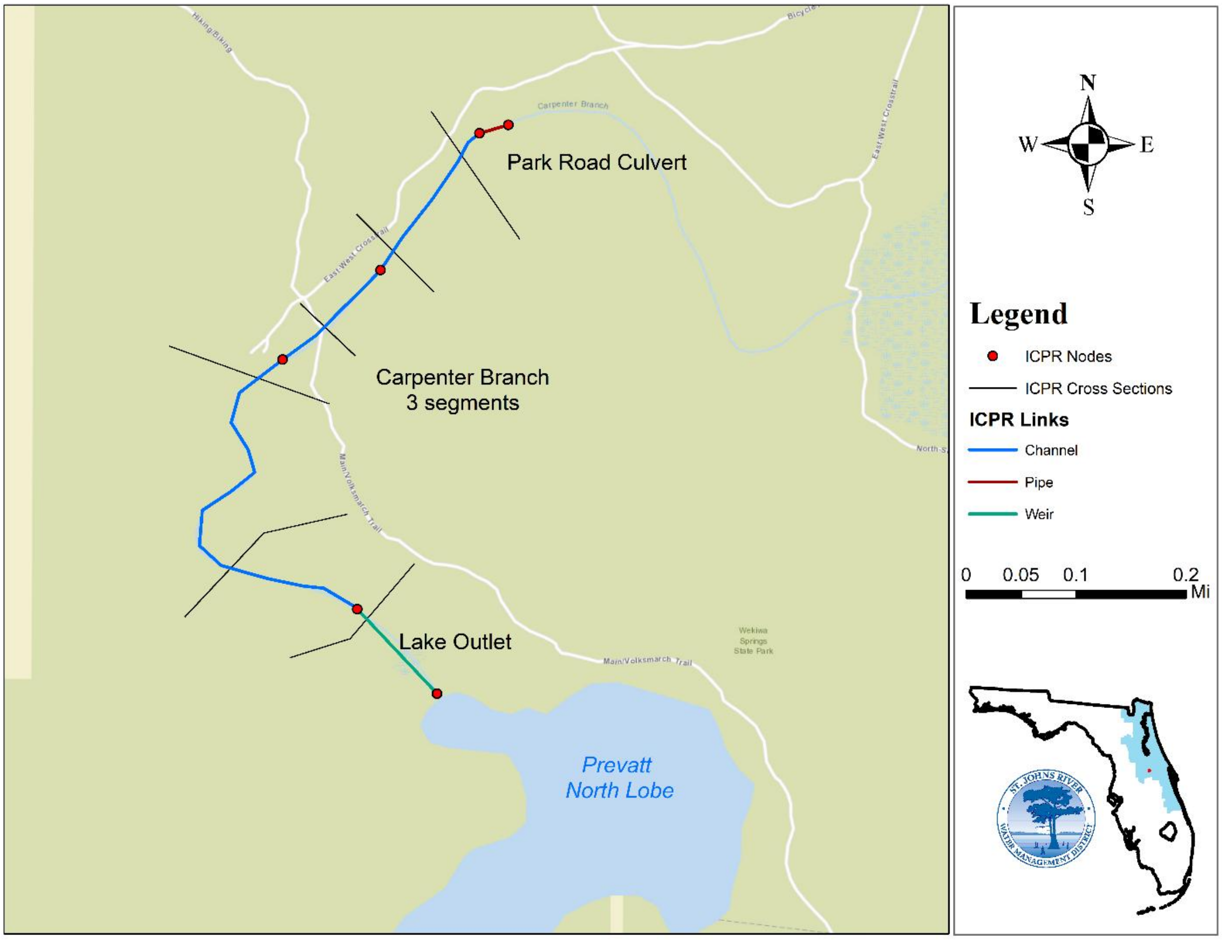

Figure 17: Schematic of ICPR model for lake stage-discharge relationship

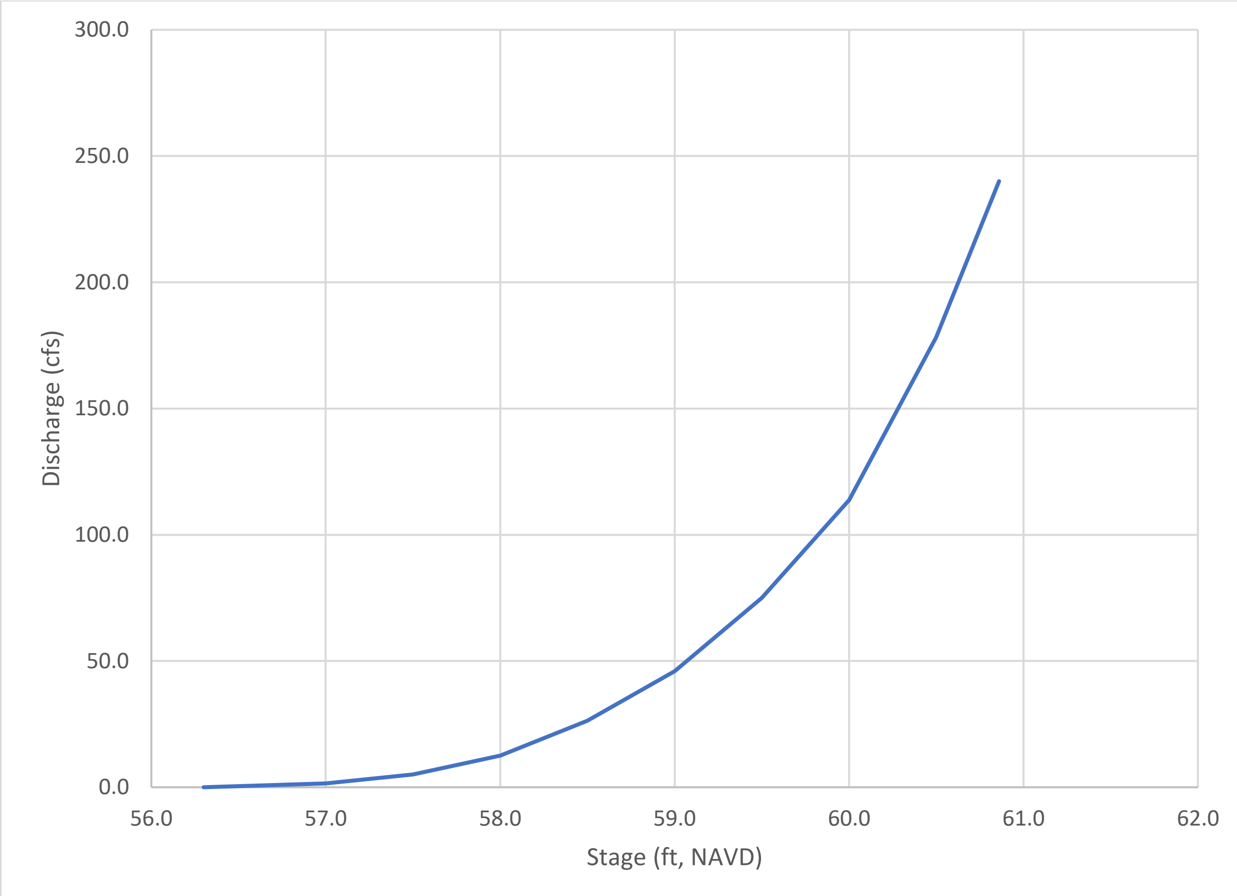

Figure 18. Lake Prevatt stage-discharge relationship

Groundwater Losses from Lake to UFA

Lake Prevatt can lose water to the UFA, with the flux dependent on the gradient between the lake's water level and the head in the UFA. The model simulated this loss using Darcy's Law:

$$Q = K\frac{\Delta H}{D}A$$

where:

$Q\ [cfs]$ is the groundwater loss flux, $K\ \left[\frac{ft}{s}\right]$ is the conductivity of the bed, $\Delta H\ [ft]$ is head difference in elevation between the lake water level and the aquifer potentiometric surface, $D\ [ft]$ is the depth of the bed material through which leakage occurs $[ft]$, and $A\ [ft^2]$ is the area of the lake bottom. The term $K/_D$ is called leakance (L) and considered in the model as a calibration parameter. The Special Actions module of HSPF was used to implement this equation.

Variable Lake Surface Area

With the rise and fall of the lake stages due to seasonal weather changes, the area of the surrounding wetland is expected to fluctuate. This variation in areal coverage of the wetlands was simulated in the model through HSPF's Special Actions as well. This method is described in Jobes, 2022.

MODEL CALIBRATION AND VALIDATION

The model was calibrated for the period from 2008 to 2020 and validated for the period from 1995 to 2007. The calibrated parameter values from the Middle St. Johns River Basin (MSJRB) HSPF model were used as a starting point for our calibration of the Lake Prevatt model, which was carried out for both the North and South Lobes of Lake Prevatt. The validation process was carried out for the North Lobe only, since the record for the South Lobe was so short. The principal focus was on matching the simulated and observed stages, and on producing a reasonable simulated water balance.

The model calibration process focused on optimizing the model parameters including LZSN, INFILT, DEEPFR, AGWETP, UZSN, LZETP, and leakance (L) value. The final calibrated values for these parameters are shown in Table 4. Except for the DEEPFR and leakance, these are watershed parameters that may vary by land cover but are the same in the two subwatersheds. DEEPFR differs between the two subwatersheds, but are the same for all land covers in each one. The calibrated leakance differs for the two lobes of the lake.

Table 4. Calibrated values for principal hydrology parameters.

Parameter	Description	Units	Calibrated Value
LZSN	Lower zone nominal soil moisture storage	inches	2.0 to 6.0 for uplands, 0.50 for wetlands.
INFILT	Index to infiltration capacity	in/hr	0.21 to 0.44 for uplands, 0.001 for wetlands.
DEEPFR	Fraction of groundwater inflow to deep recharge	none	0.35 for North Lobe watershed 0.15 for South Lobe watershed
AGWETP	Fraction of remaining ET from active groundwater	none	0.0 for uplands, 0.9 for wetlands.
UZSN	Upper zone nominal soil moisture storage	inches	0.20 to 0.60 for uplands. 0.10 for wetlands.
LZETP	Lower zone ET parameter	none	0.23 to 0.89 for uplands, 0.90 for wetlands.
L	Leakance parameter	/day	0.0023 to 0.0060 for North Lobe, 0.0023 to 0.0250 for South Lobe.

Lake Stages

The North Lobe simulated stages generally matched the observed stages in terms of temporal variations during the calibration period, shown in Figure 19, along with the groundwater boundary condition. In general, the modeled stage closely followed the shape of the groundwater head timeseries. Performance metrics for the calibrated stages versus the observed stages are in Table 5. The model tended to underestimate the wet season in the dry years 2011-2013 and overestimate the response to Hurricane Matthew in 2016. The model response seems reasonable given the rainfall data, however. For instance, in the 2011-2013 the rainfall data remains low in intensity throughout the wet season. Due to the lack of local rain gauges, the accuracy of NEXRAD data cannot be confirmed at this level of temporal and spatial detail. A comparison of the exceedance probability curves in Figure 20 showed good agreement across most of the range, with a small period of undersimulation around a stage of 51 feet and tendency to over-simulate slightly in the lowest 10%. Nonetheless, the model simulated stage well for the North Lobe during the calibration period.

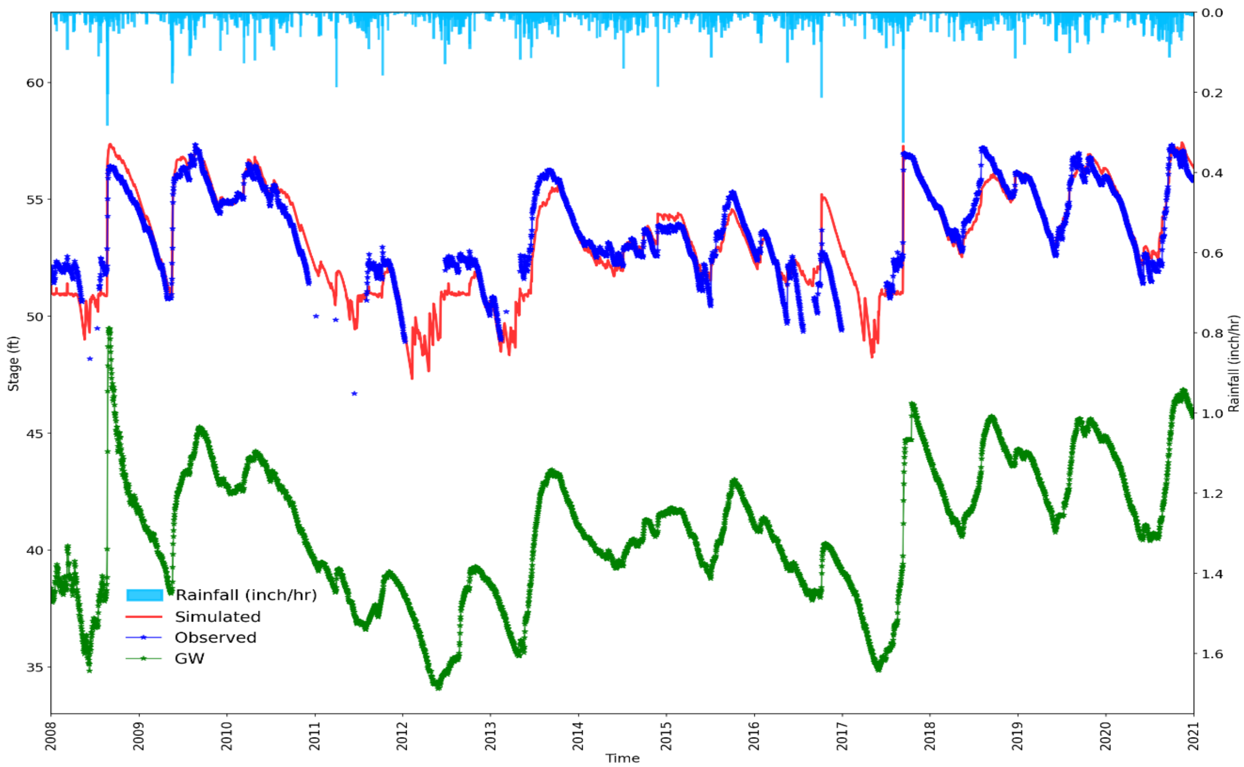

Figure 19. Observed and simulated daily stages for the North Lobe of Lake Prevatt for calibration period (ft NAVD88)

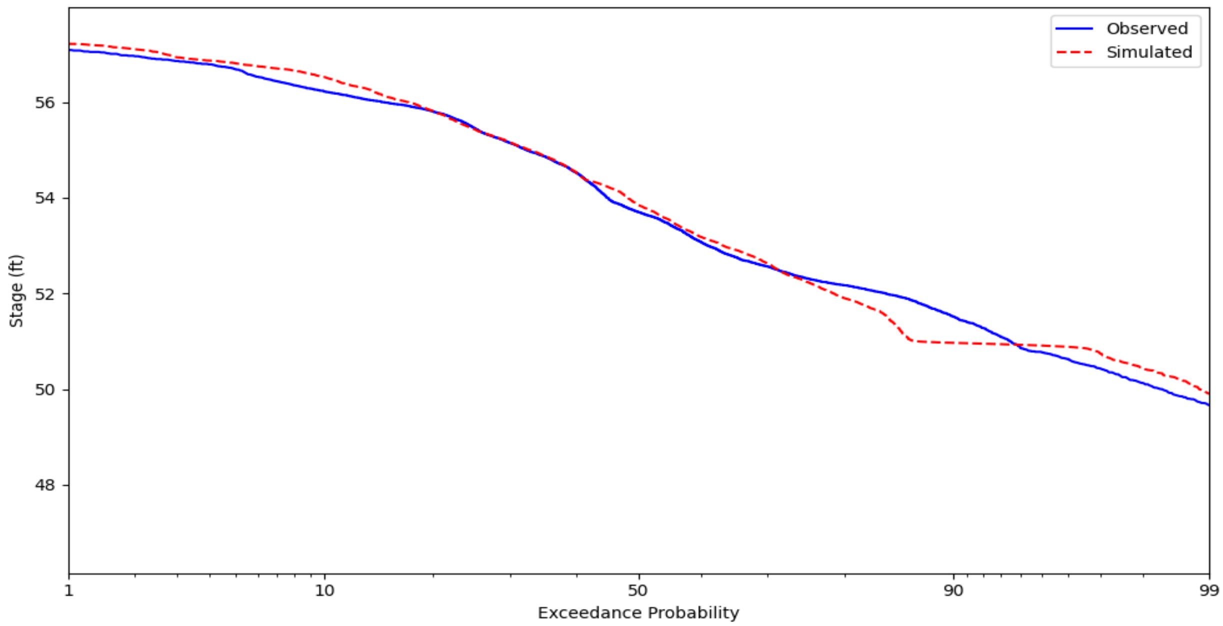

Figure 20. Observed and simulated daily exceedance probability curves for North Lobe for calibration period (ft NAVD88)

Because the record of South Lobe observed daily stage is only available from 2022 to present, the extended and adjusted South Lobe data described above (Figure 10) was used for calibration. The simulated stages generally matched with the extended observed stage data for the calibration period, as seen in Figure 21. The adjusted data show a significant drop in the 2016-2018 period which is consistent with the groundwater level. The model overestimated the periods in early 2009 and 2016-2017, while in the 2011-2013 period the simulated is similar to the observed but the timing is off. The simulated and observed exceedance probability curves in Figure 22 showed a good agreement throughout but especially during high stages, and the model slightly over-simulated the lowest 10% of stages, similarly to the North Lobe, though the highest oversimulation is around 52 feet. Overall, the South Lobe simulated stage is adequately modeled in the calibration period.

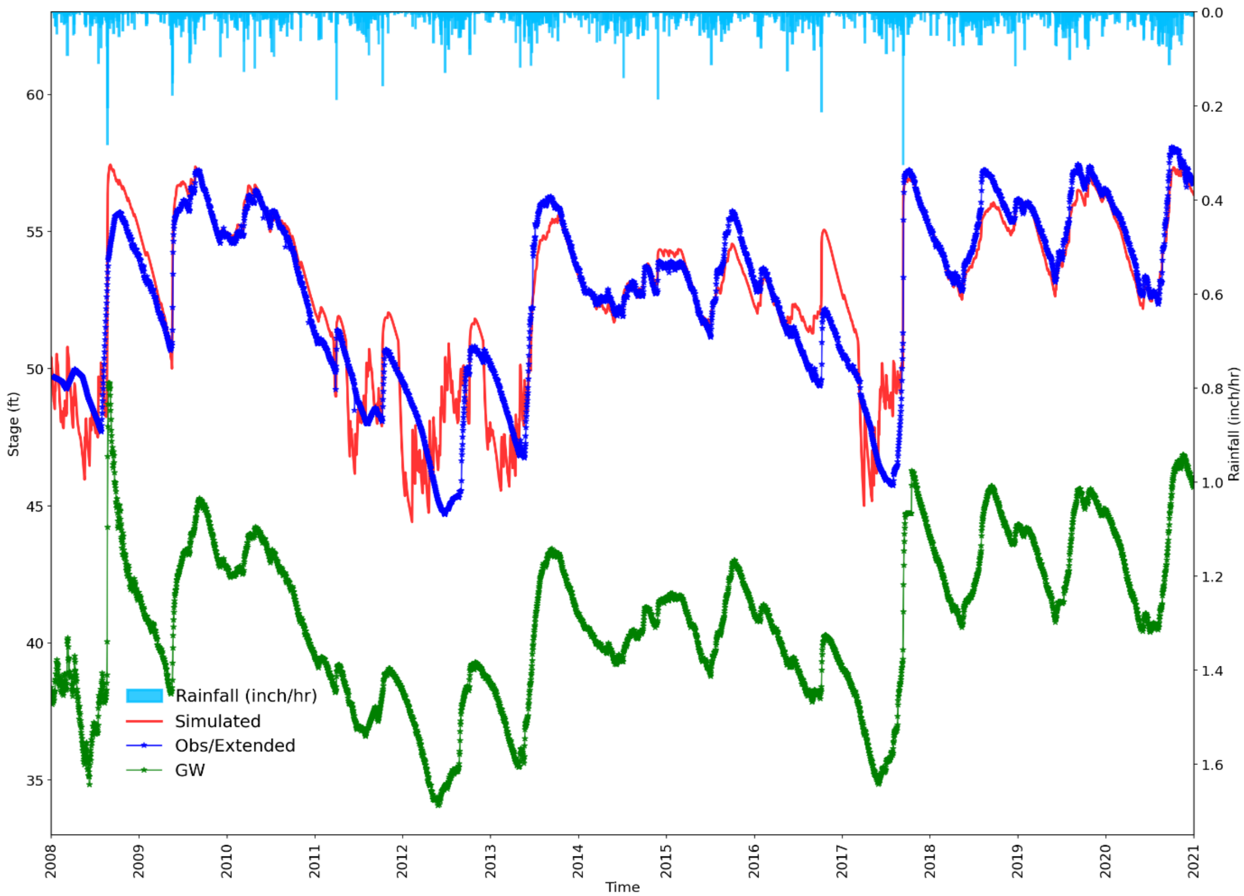

Figure 21. Observed/extended and simulated daily stages for the South Lobe of Lake Prevatt for calibration period (ft NAVD88)

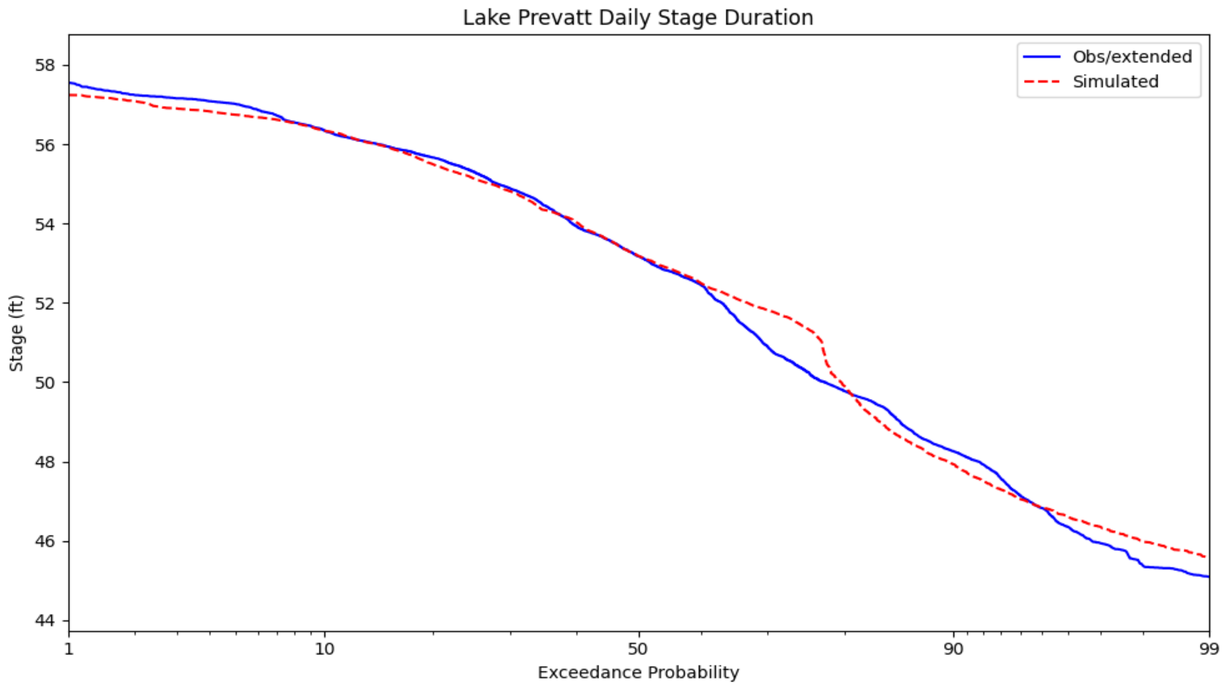

Figure 22. Observed and simulated daily exceedance probability curves for South Lobe for calibration period (ft NAVD88)

The model was validated for a period from 1995 to 2007. The model was validated only for the North Lobe due to the lack of observed stage data for the South Lobe during this time. In general, as seen in Figure 23, the simulated stages match well with the observed stages in terms of temporal variations during the latter part of the validation period where daily observations were available. In the earlier part of the period, when the observations are sparse, the model did not reproduce the lower stages well. The exceedance probability curve comparison in Figure 24 shows reasonably good agreement throughout the full range of plotted probabilities, with only a slight over-simulation of high stages and under-simulation at low stages. Thus, even with these limitations, the model adequately simulated stage for the North Lobe during the validation period.

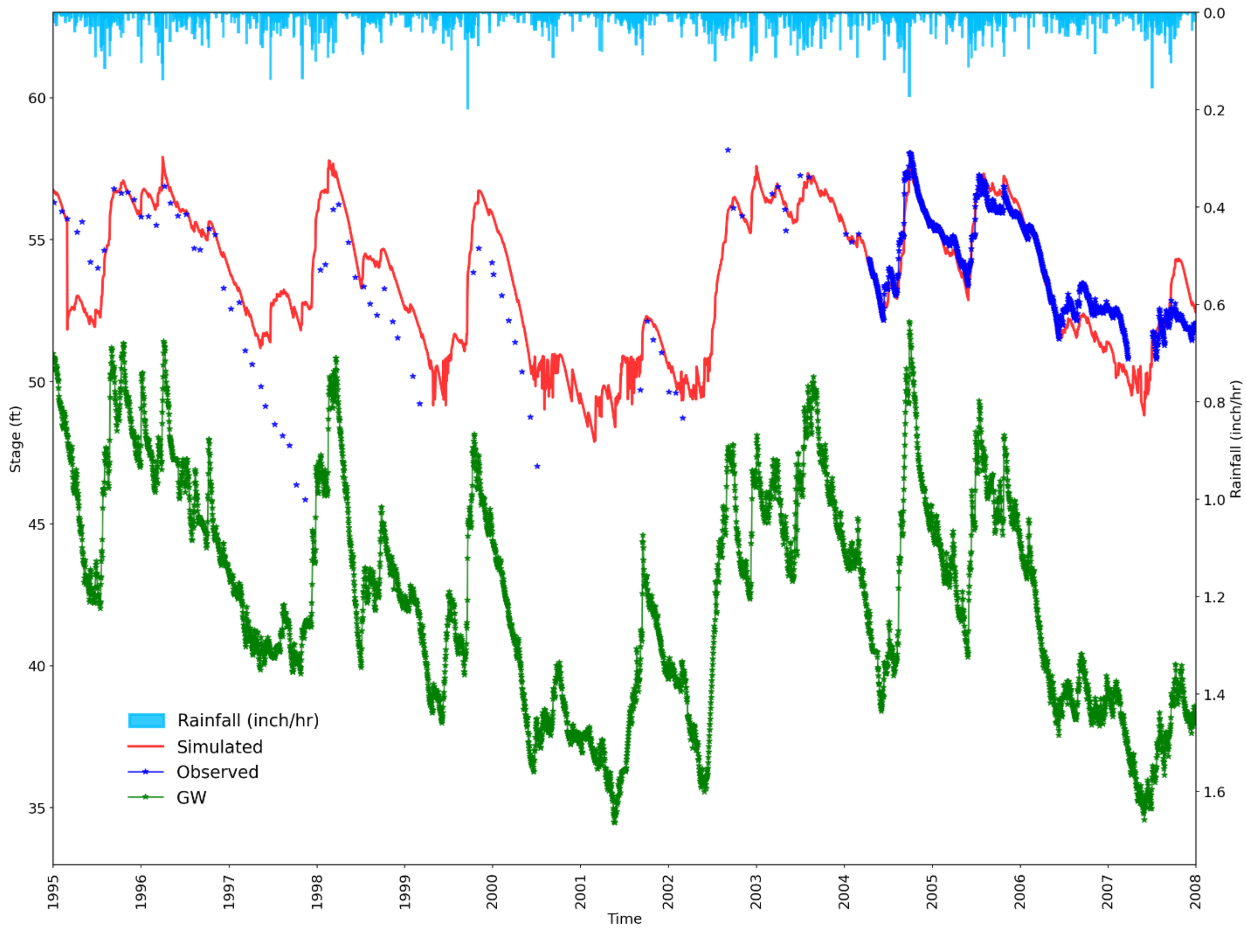

Figure 23. Observed and simulated daily stages for the North Lobe of Lake Prevatt for validation period (ft NAVD88)

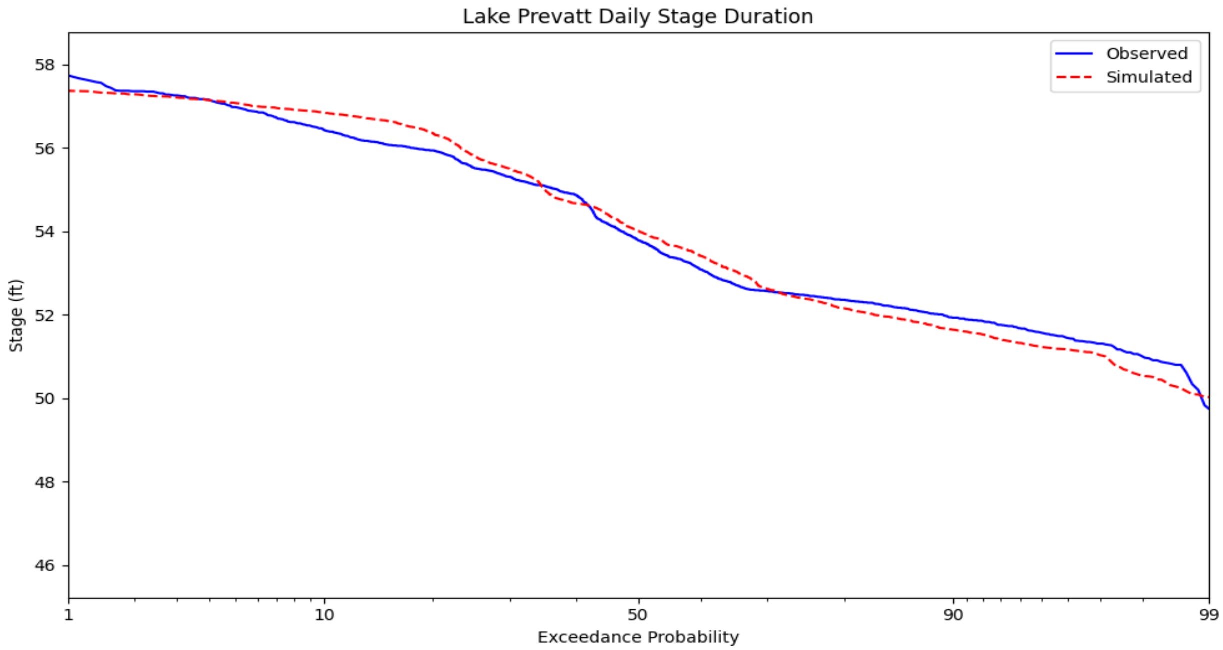

Figure 24. Observed and simulated daily exceedance probability curves for North Lobe for validation period (ft NAVD88)

The detailed calibration and validation statistics for the North and South Lobes are shown in Table 5 and Table 6 respectively. For the North Lobe, all targeted values were achieved for both the calibration and validation periods, while for the South Lobe, where the extended “observations” are more uncertain, four of six targeted values were achieved. Given this limitation in the data, the model performed reasonably well in matching the simulated stages to the available observations.

Table 5. Goodness-of-fit statistics for daily North Lobe stages simulation

Statistics			**Prevatt North Lobe Statistics**	
Description	Symbol	Target value	Calibration	Validation
Nash-Sutcliffe Efficiency	NSE	≥0.8 (cal) & 0.7 (val)	0.83	0.76
Root Mean Squared Error	RMSE	$\leq \lvert \pm 1 \rvert$ ft	0.76	0.92
Mean Error	ME	$\leq \lvert \pm 1 \rvert$ ft	0.01	0.10
Percent Bias	PBIAS	$\leq \lvert \pm 10\% \rvert$ (cal) & $\lvert \pm 15\% \rvert$ (val)	0.02%	0.19%
Pearson Correlation Coefficient	R	≥0.8 (cal) & 0.7 (val)	0.92	0.89
Percent of observations bracketed within ± 1ft	±1ft (%)	≥ 85% (cal) & 70% (val)	83.94%	80.97%

Table 6. Goodness-of-fit statistics for daily South Lobe stages simulation

Statistics			Prevatt South Lobe Statistics	
Description	Symbol	Target value	Calibration	Validation
Nash-Sutcliffe Efficiency	NSE	≥0.8 (cal) & 0.7 (val)	0.83	N/A Due to lack of observed data
Root Mean Squared Error	RMSE	≤ |±1| ft	1.29	
Mean Error	ME	≤ |±1| ft	0.07	
Percent Bias	PBIAS	≤ |±10%| (cal) & |±15%| (val)	0.14%	
Pearson Correlation Coefficient	R	≥0.8 (cal) & 0.7 (val)	0.91	
Percent of observations bracketed within ± 1ft	±1ft (%)	≥85% (cal) & 70% (val)	68.94%	

Water Balance

Annual averages of the simulated water balance components, such as actual evapotranspiration (ET), surface runoff, baseflow, and recharge to UFA were assessed for both the calibration and validation periods. The values are reported for these two periods respectively in Table 7 and Table 8 for each model land cover category. Simulated evapotranspiration accounted for more than 50% of the annual water balance, and the values for each category were close to target values developed by SJRWMD (Jobes, T., 2022). The recharge to the UFA was within the bounds of SJRWMD estimates of long-term average values (Boniol and Mouyard, 2016). Overall, the simulated water balance components were reasonable.

Table 7. Annual average water budget for the calibration period per land-use in inches per year

Description	LDR	MDR	HDR	CI	OPN	AGR	RNG	FRS	WTL	Watershed
Rainfall	51.1	51.1	51.1	51.1	51.1	51.1	51.1	51.1	51.1	51.1
Evapotranspiration	35.5	33.1	28.3	24.7	28.0	39.9	38.4	42.4	48.7	37.2
Total runoff	12.9	16.1	20.1	24.5	20.5	7.9	8.9	6.3	0.8	11.7
Baseflow	9.3	10.0	8.1	8.4	17.5	7.0	7.6	6.0	0.7	6.9
Recharge to UFA	3.1	2.5	4.3	4.1	3.1	3.5	4.1	2.4	0.6	2.3

Table 8. Annual average water budget for the validation period per land-use in inches per year

Description	LDR	MDR	HDR	CI	OPN	AGR	RNG	FRS	WTL	Watershed
Rainfall	47.7	47.7	47.7	47.7	47.7	47.7	47.7	47.7	47.7	47.7
Evapotranspiration	33.4	31.2	26.7	23.3	26.5	37.5	36.1	39.6	46.1	35.0
Total runoff	11.7	14.8	18.5	22.6	18.7	7.1	7.9	5.9	1.0	10.7
Baseflow	9.0	9.7	7.8	8.1	16.6	6.8	7.4	5.8	0.7	6.7
Recharge to UFA	3.0	2.4	4.2	3.9	2.9	3.4	4.0	2.4	0.6	2.2

Table 9 and

Table 10 summarize the annual average water budgets for the North and South Lobes of Lake Prevatt for both the calibration and validation periods. The tables indicate that seepage to groundwater dominate the outflow components of the lake. Higher surface outflows from the North Lobe are simulated during the validation period, due to the higher average direct rainfall compared to the calibration period.

Table 9. Annual average water budget for North Lobe in acre-feet

Period	Direct Rain	Water - shed Inflow	Flow from South	Total Inflow	ET	GW Loss	Outfal l	Flow to South	Total Outflo w
Calibration	62.6	457.5	24.2	544.4	60.1	172.8	64.0	241.6	538.4
Percent	11.5	84.1	4.5	-	11.0	31.7	11.7	44.4	-
Validation	67.4	420.8	74.8	563.1	64.0	158.2	162.4	176.5	561.1
Percent	12.0	74.7	13.3	-	11.4	28.1	28.8	31.3	-

Table 10. Annual average water budget for South Lobe in acre-feet

Period	Direct Rain	Water -shed Inflow	Flow from North	Total Inflow	ET	GW Loss	Flow to North	Total Outflo w
Calibration	220.1	529.3	241.6	990.9	218.9	719.3	24.2	962.4
Percent	22.2	53.4	24.4	-	22.1	72.6	2.4	-
Validation	236.3	487.0	176.5	899.9	229.1	587.0	74.8	890.9
Percent	26.3	54.1	19.6	-	25.5	65.2	8.3	-

SENSITIVITY ANALYSIS

We performed model sensitivity analysis using a one-factor-at-a-time method, which is commonly called the “local” method (Saltelli et al., 2004; Campolongo et al., 2010). This method varies one model input parameter value at a time from the calibrated value while other model input parameter values are kept constant. Using this method, we evaluated the importance of certain HSPF parameters on the simulated stages of Lake Prevatt.

We compared and investigated the sensitivity of five selected parameters: leakance (L), lower zone nominal storage (LZSN), the fraction of recharge that becomes inactive groundwater inflow (DEEPFR), lower zone ET parameter (LZETP), and infiltration index (INFILT). The leakance was varied by factors of 2 and 3, while the rest of parameters were varied by increasing and decreasing by 10% and 20%. The timeseries and performance metrics from these runs were compared to the original model results for the calibration period. The resulting goodness-of-fit statistics are summarized in Table 11 and Table 12 for North Lobe and South Lobe, respectively. Figure 25 through Figure 34 show time series plots and comparison plots of exceedance probability curves for each parameter for each lobe.

We found that the leakance, which controls the UFA flux to or from the lake, was the most sensitive/important parameter for Lake Prevatt. In contrast, increasing or decreasing the LZSN, DEEPFR and INFILT values by 10 or 20% made only relatively small changes to the simulated stages. LZETP showed some impact on simulated stages, but not as strongly as the leakance.

Table 11. Impact on model goodness-of-fit statistics compared to calibrated values for North Lobe

Parameter	Calibrated value	Calibration statistics			Sensitivity statistics			Absolute change		
		NSE	RMSE	PBIAS	NSE	RMSE	PBIAS	NSE	RMSE	PBIAS
Leakance	Divided by 2	0.83	0.76	0.02	-0.68	2.41	3.79	-1.52	1.65	3.77
	Divided by 3				-1.47	2.92	4.65	-2.30	2.16	4.63
	Multiplied by 2				-1.30	2.82	-4.51	-2.13	2.06	-4.53
	Multiplied by 3				-2.84	3.64	-6.06	-3.67	2.88	-6.08
LZSN	Decreased by 20%	0.83	0.76	0.02	0.80	0.83	0.31	-0.03	0.07	0.29
	Decreased by 10%				0.83	0.77	0.06	0	0.01	0.04
	Increased by 10%				0.82	0.78	-0.08	-0.01	0.02	-0.10
	Increased by 20%				0.82	0.78	-0.12	-0.01	0.02	-0.14
DEEPFR	Decreased by 20%	0.83	0.76	0.02	0.82	0.78	0.20	-0.01	0.02	0.18
	Decreased by 10%				0.83	0.77	0.09	0	0.01	0.07
	Increased by 10%				0.81	0.80	-0.19	-0.02	0.04	-0.21
	Increased by 20%				0.81	0.81	-0.27	-0.02	0.05	-0.29
LZETP	Decreased by 20%	0.83	0.76	0.02	0.72	0.98	0.79	-0.11	0.22	0.77
	Decreased by 10%				0.78	0.86	0.46	-0.05	0.10	0.44
	Increased by 10%				0.81	0.80	-0.34	-0.02	0.04	-0.36
	Increased by 20%				0.81	0.81	-0.66	-0.02	0.05	-0.68
INFILT	Decreased by 20%	0.83	0.76	0.02	0.83	0.77	-0.04	0	0.01	-0.06
	Decreased by 10%				0.83	0.76	-0.01	0	0	-0.03
	Increased by 10%				0.81	0.80	-0.05	-0.02	0.04	-0.07
	Increased by 20%				0.81	0.80	0.01	-0.02	0.04	-0.01

Table 12. Impact on model goodness-of-fit statistics compared to calibrated values for South Lobe

Parameter	Calibrated value	Calibration statistics			Sensitivity statistics			Absolute change		
		NSE	RMSE	PBIAS	NSE	RMSE	PBIAS	NSE	RMSE	PBIAS
Leakance	Divided by 2	0.83	1.29	0.14	-0.32	3.59	5.38	-1.15	2.30	5.24
	Divided by 3				-0.84	4.24	6.46	-1.66	2.94	6.32
	Multiplied by 2				-0.79	4.18	-6.28	-1.62	2.89	-6.42
	Multiplied by 3				-1.94	5.36	-8.62	-2.77	4.07	-8.76
LZSN	Decreased by 20%	0.83	1.29	0.14	0.77	1.49	0.59	-0.06	0.20	0.45
	Decreased by 10%				0.83	1.30	0.19	0	0.01	0.06
	Increased by 10%				0.82	1.33	-0.02	-0.01	0.04	-0.16
	Increased by 20%				0.82	1.32	-0.07	-0.01	0.03	-0.21
DEEPFR	Decreased by 20%	0.83	1.29	0.14	0.83	1.29	0.34	0	0	0.20
	Decreased by 10%				0.83	1.29	0.22	0	0	0.08
	Increased by 10%				0.81	1.37	-0.18	-0.02	0.08	-0.31
	Increased by 20%				0.81	1.38	-0.26	-0.02	0.09	-0.39
LZETP	Decreased by 20%	0.83	1.29	0.14	0.74	1.58	1.21	-0.09	0.29	1.08
	Decreased by 10%				0.77	1.50	0.76	-0.06	0.21	0.62
	Increased by 10%				0.80	1.39	-0.37	-0.03	0.09	-0.50
	Increased by 20%				0.78	1.46	-0.91	-0.05	0.17	-1.04
INFILT	Decreased by 20%	0.83	1.29	0.14	0.83	1.30	0.08	0	0.01	-0.06
	Decreased by 10%				0.83	1.30	0.11	0	0.01	-0.03
	Increased by 10%				0.81	1.37	-0.02	-0.02	0.08	-0.16
	Increased by 20%				0.81	1.36	0.04	-0.02	0.07	-0.10

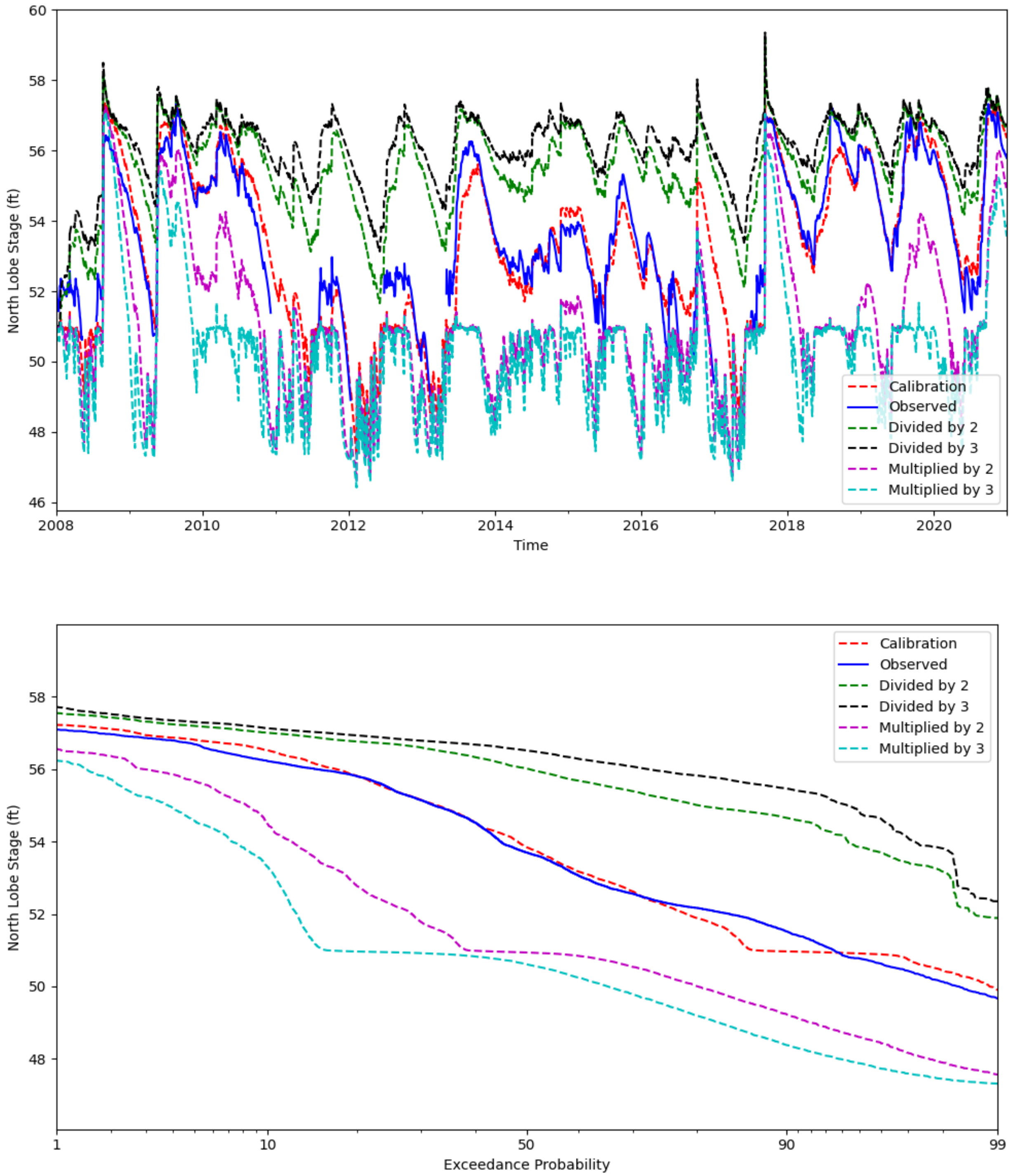

Figure 25. Impact of leakance value on simulated stages of the North Lobe of Lake Prevatt (ft NAVD88)

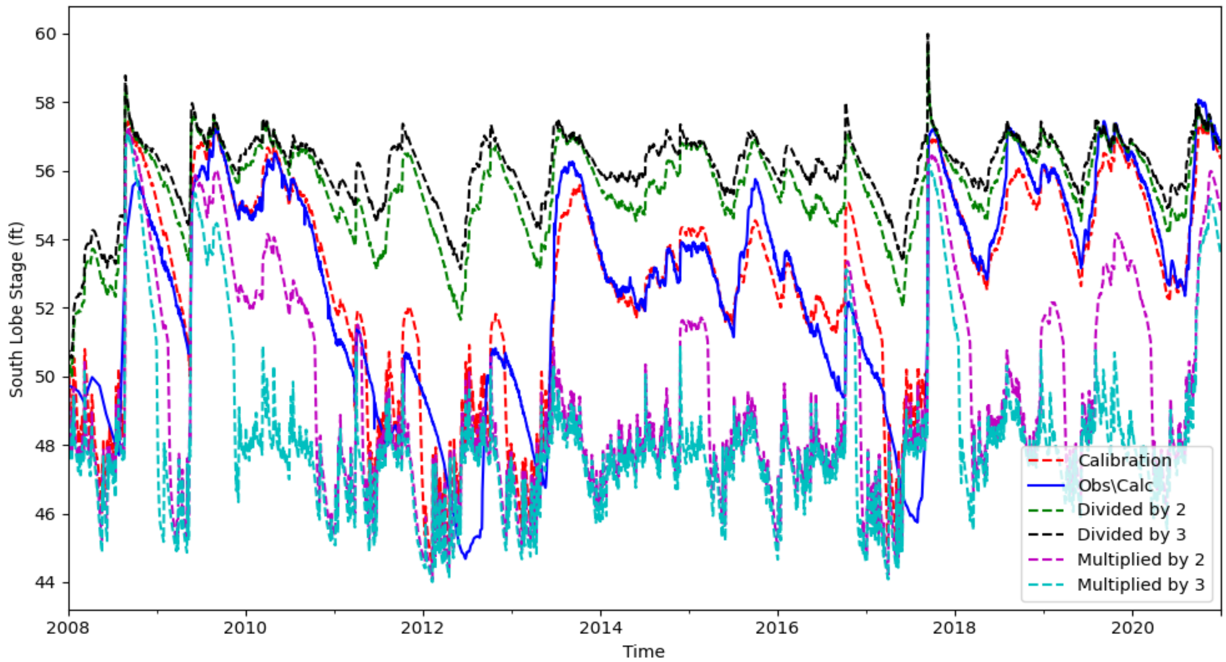

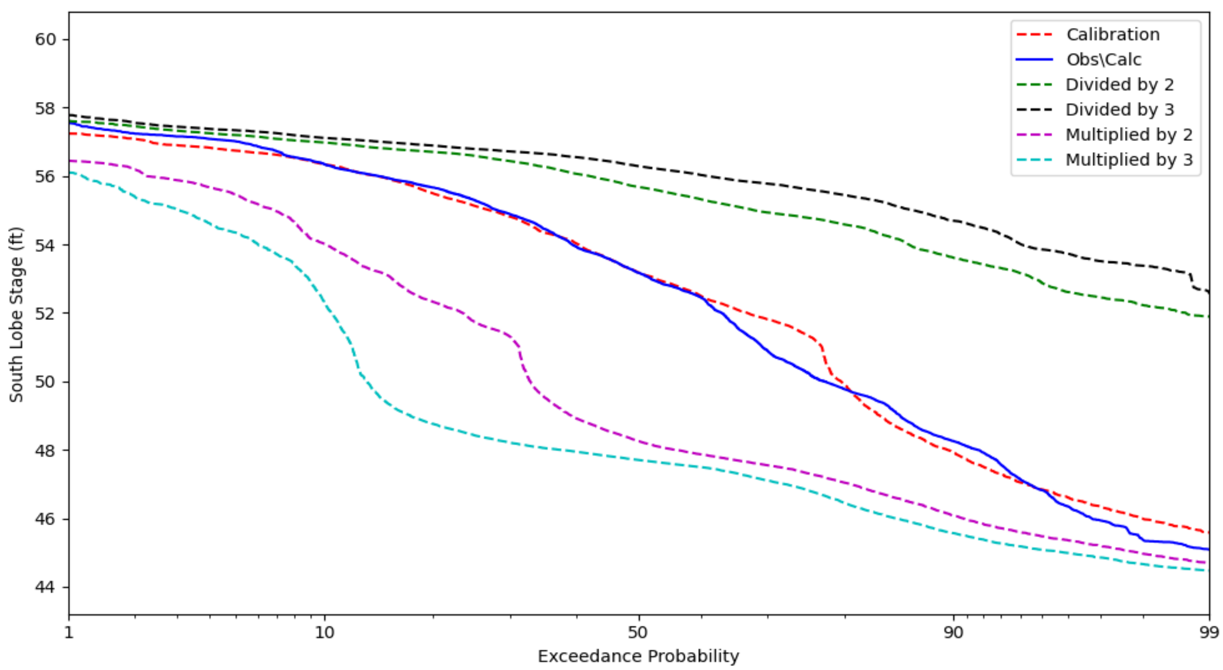

Figure 26. Impact of leakance value on simulated stages of the South Lobe of Lake Prevatt (ft NAVD88)

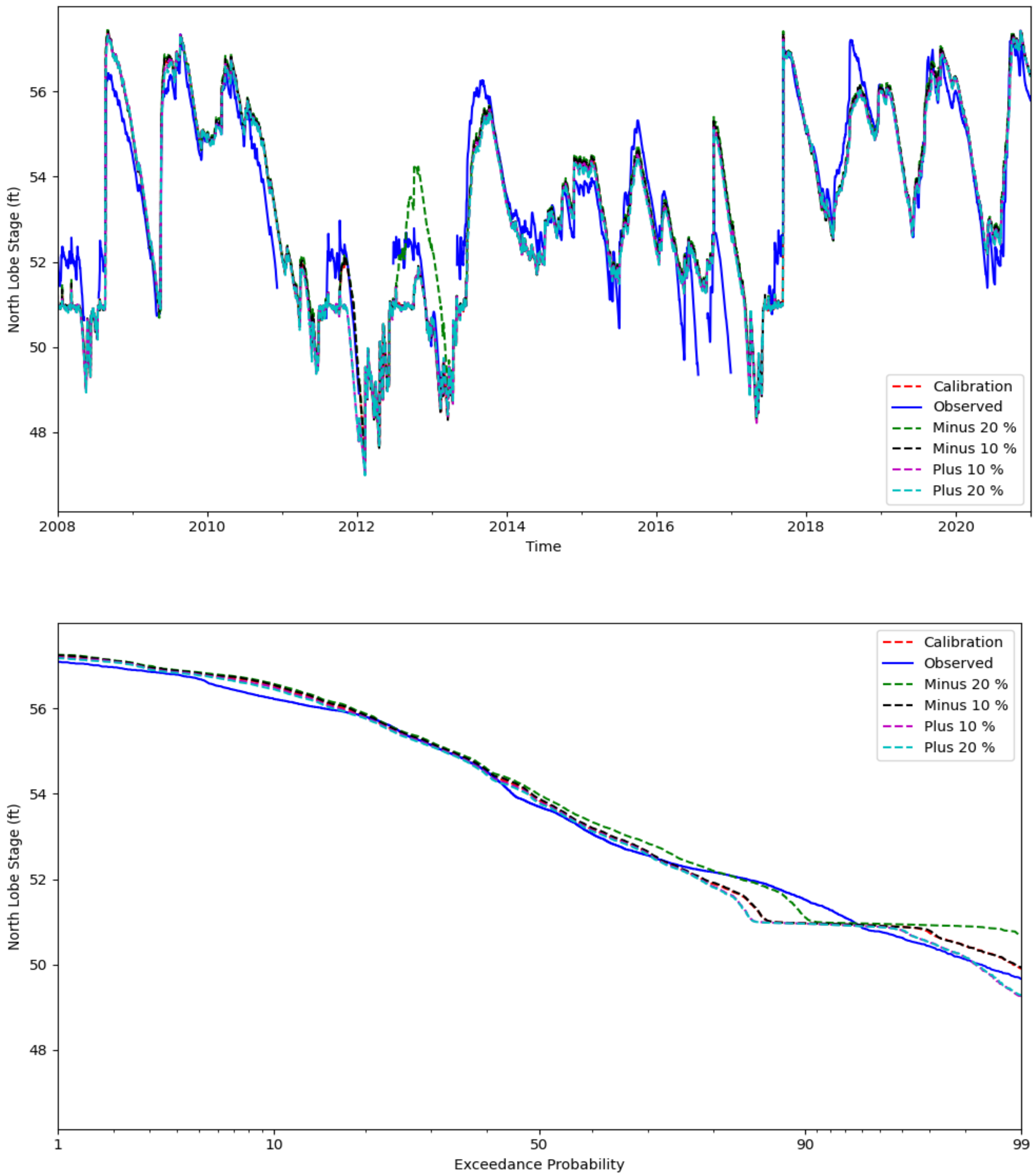

Figure 27. Impact of LZSN on simulated stages of the North Lobe of Lake Prevatt (ft NAVD88)

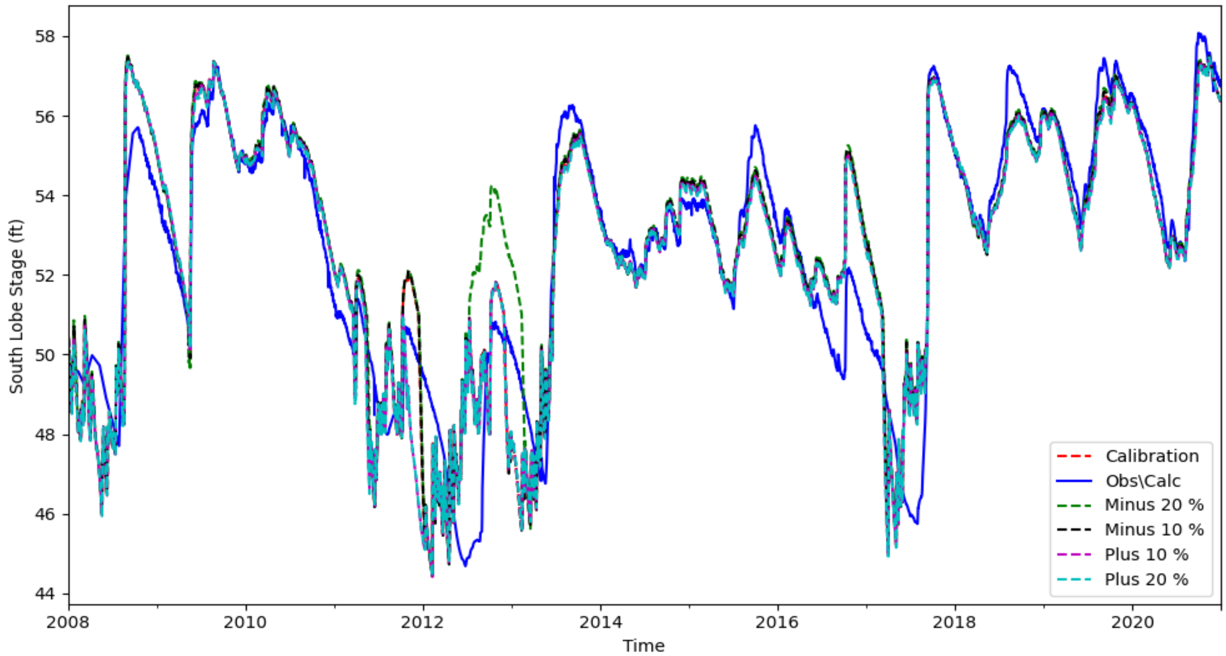

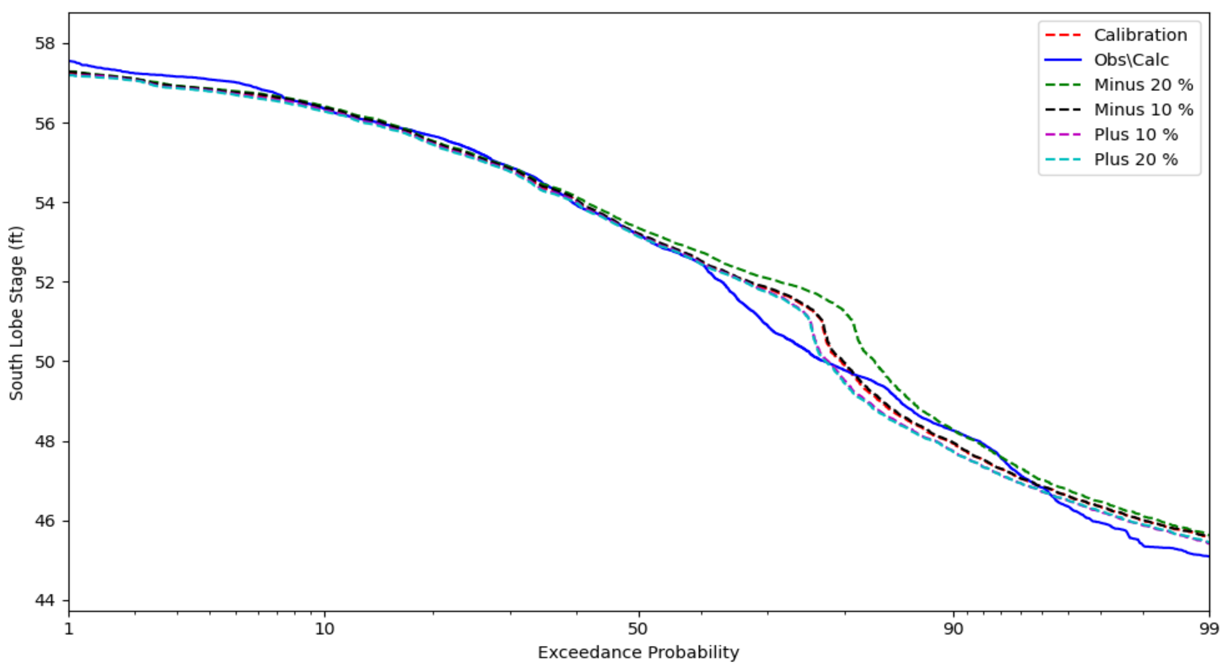

Figure 28. Impact of LZSN on simulated stages of the South Lobe of Lake Prevatt (ft NAVD88)

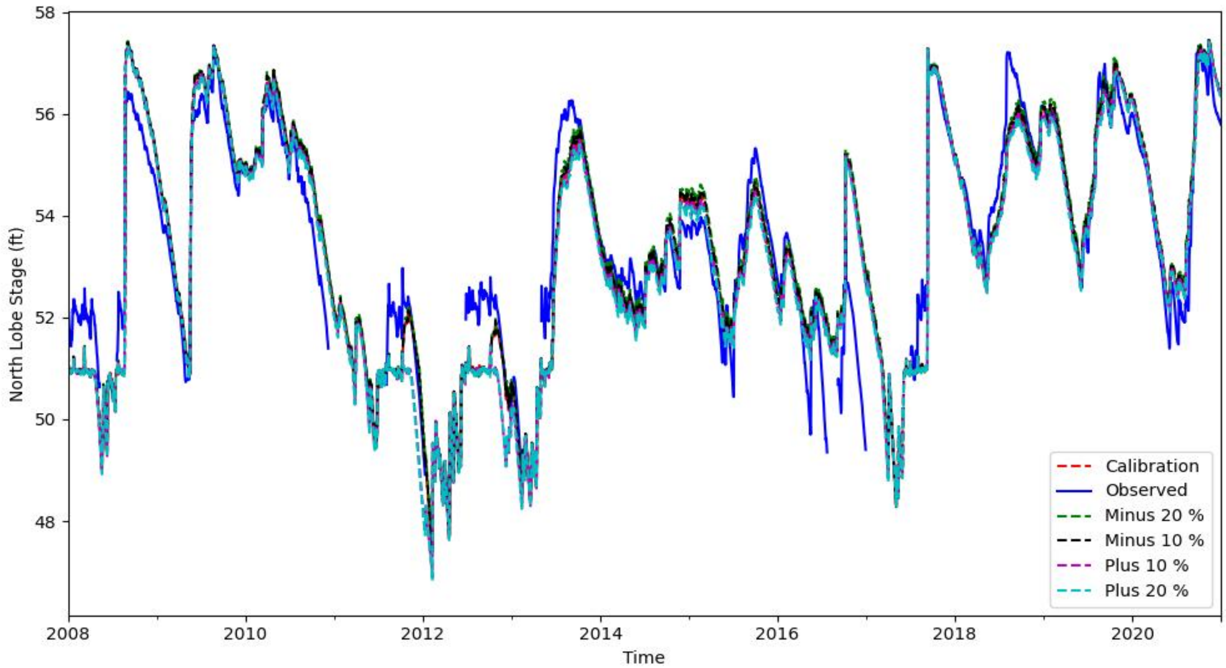

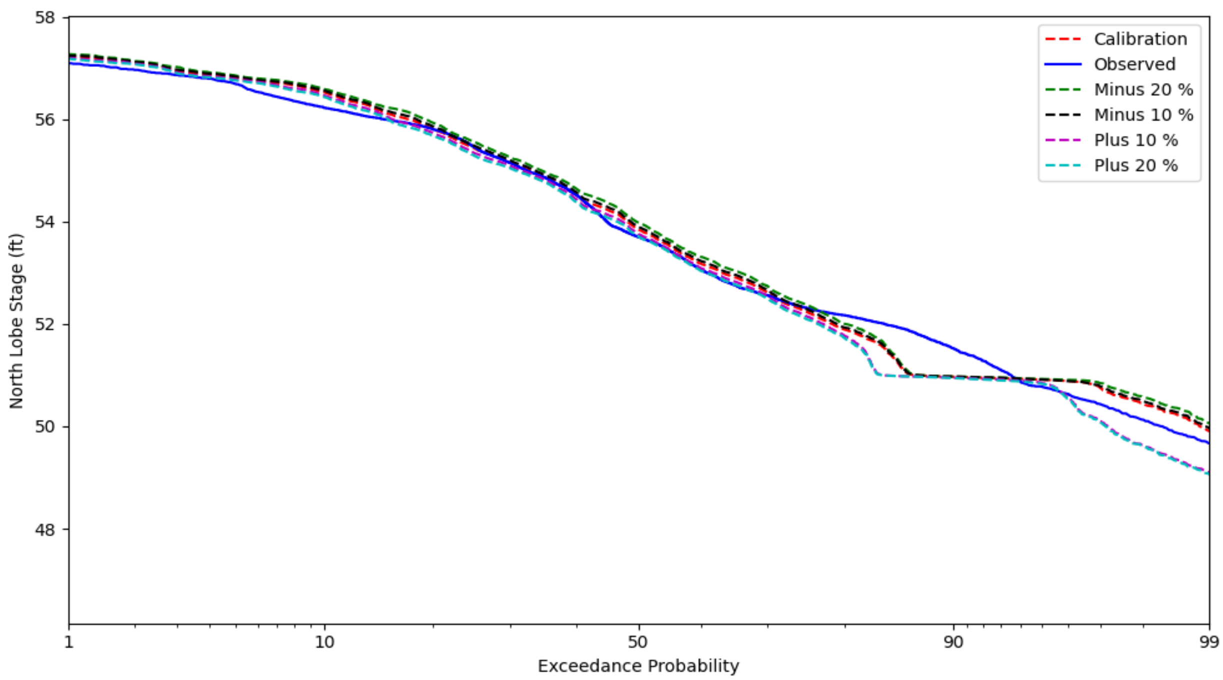

Figure 29. Impact of DEEPFR on simulated stages of the North Lobe of Lake Prevatt (ft NAVD88)

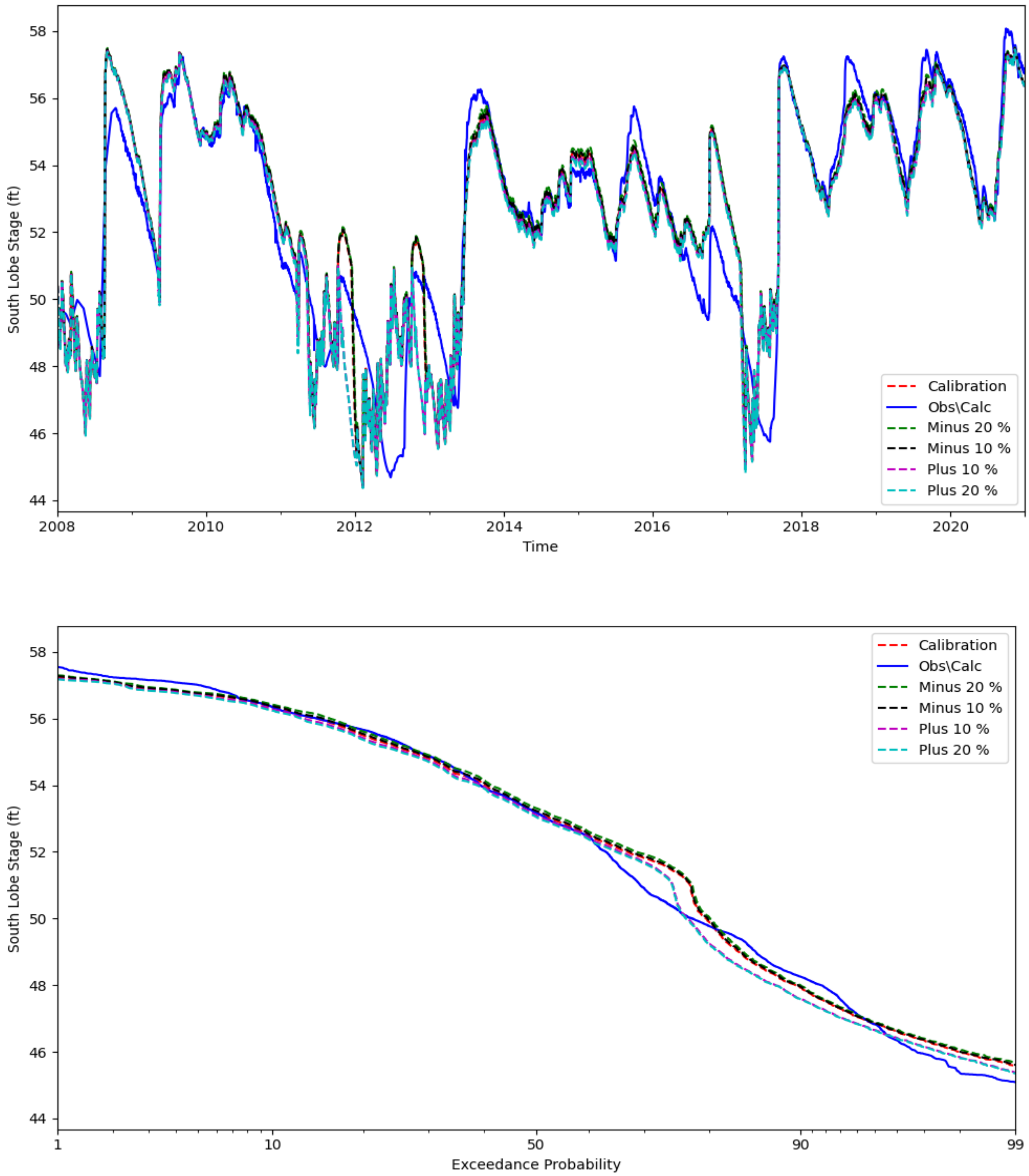

Figure 30. Impact of DEEPFR on simulated stages of the South Lobe of Lake Prevatt (ft NAVD88)

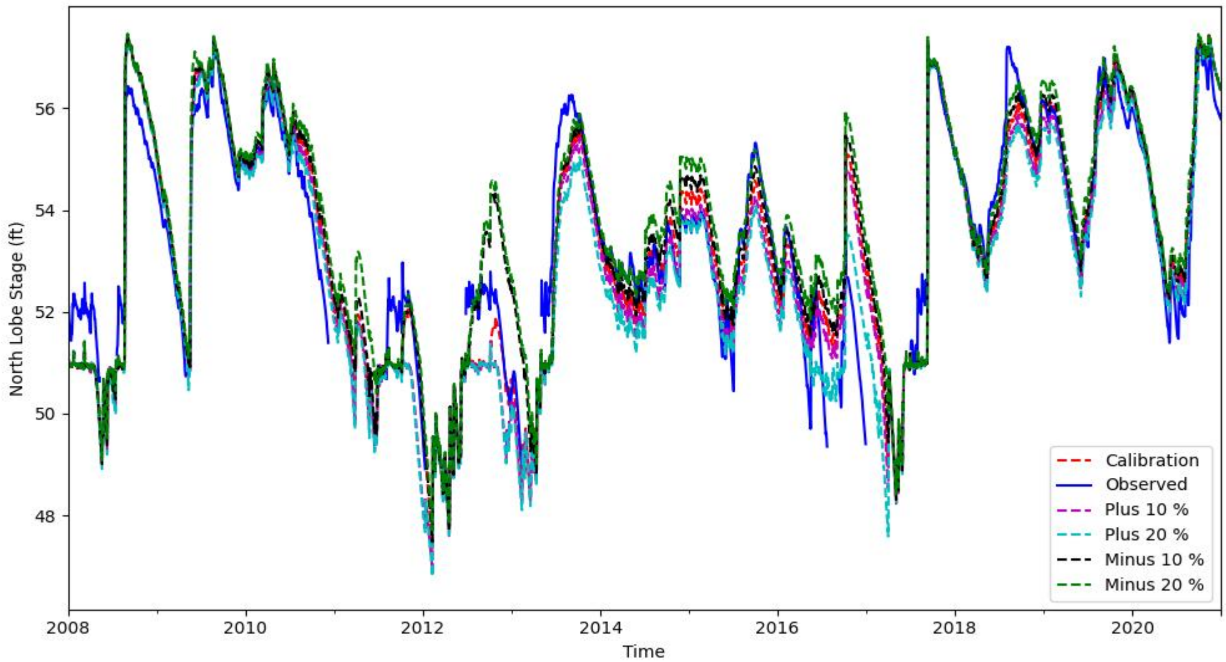

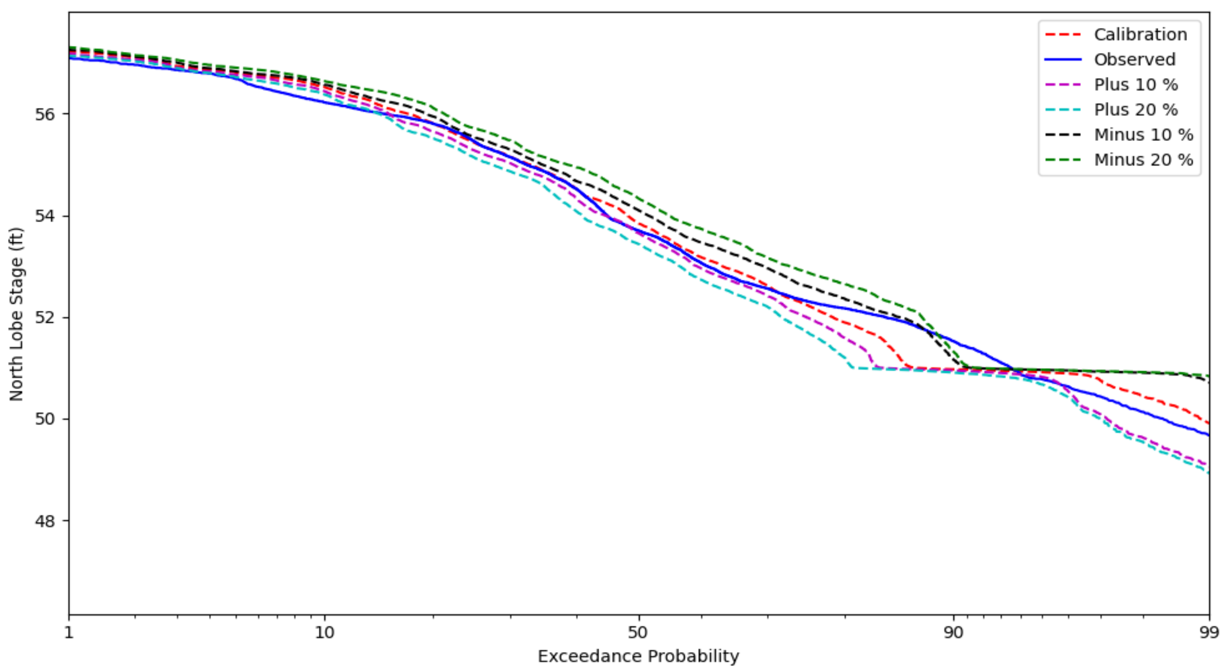

Figure 31. Impact of LZETP on simulated stages of the North Lobe of Lake Prevatt (ft NAVD88)

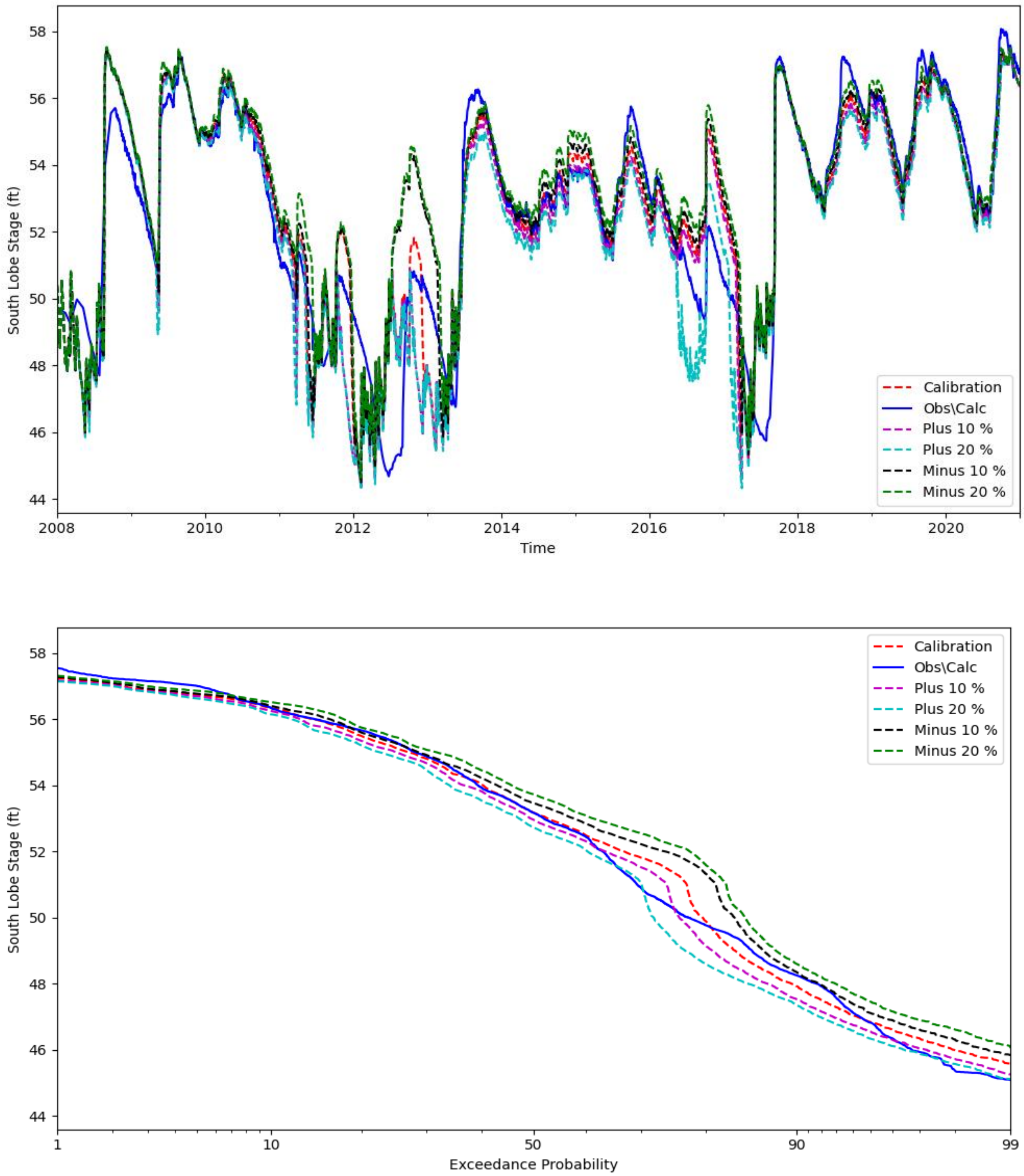

Figure 32. Impact of LZETP on simulated stages of the South Lobe of Lake Prevatt (ft NAVD88)

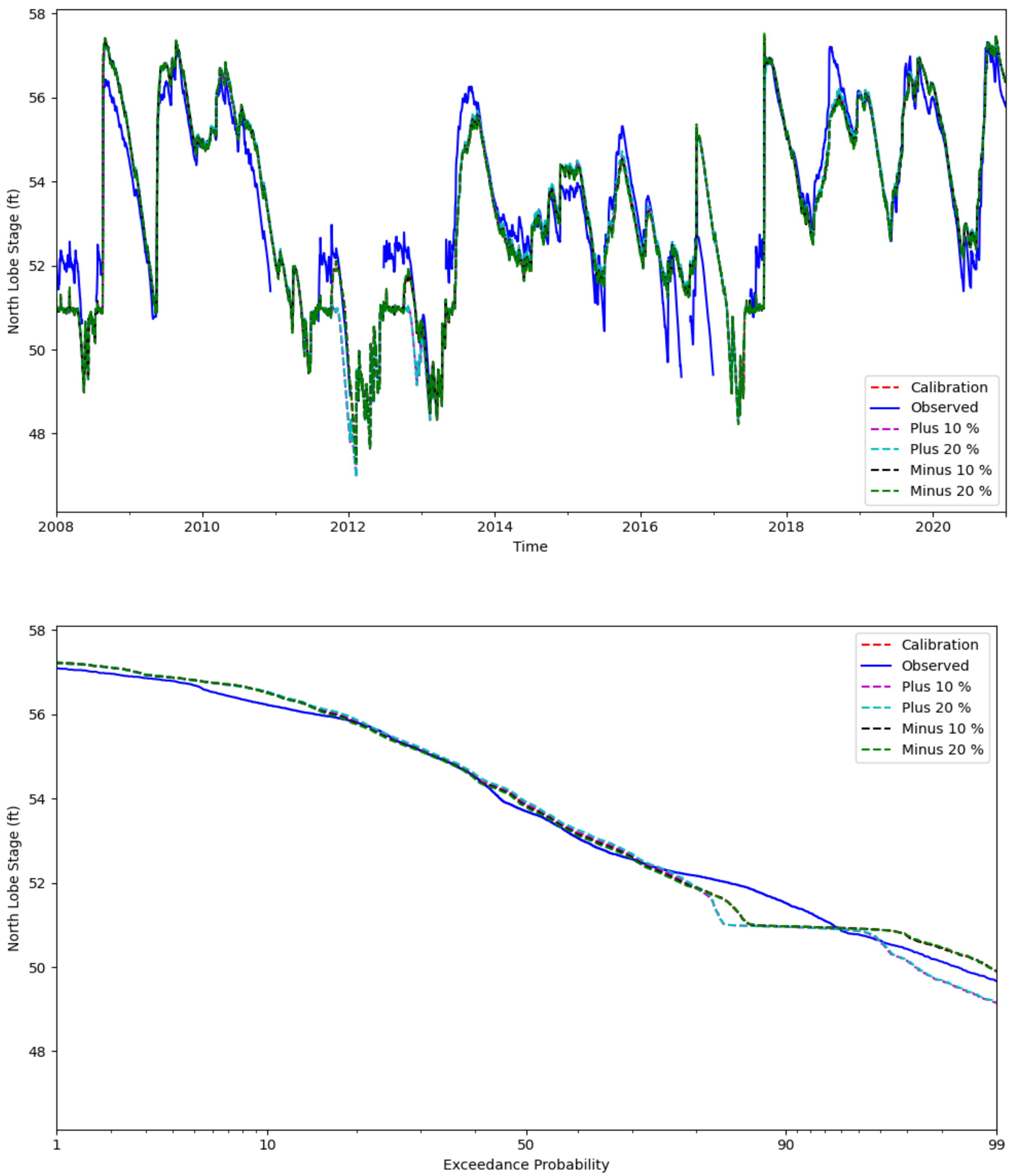

Figure 33. Impact of INFILT on simulated stages of the North Lobe of Lake Prevatt (ft NAVD88)

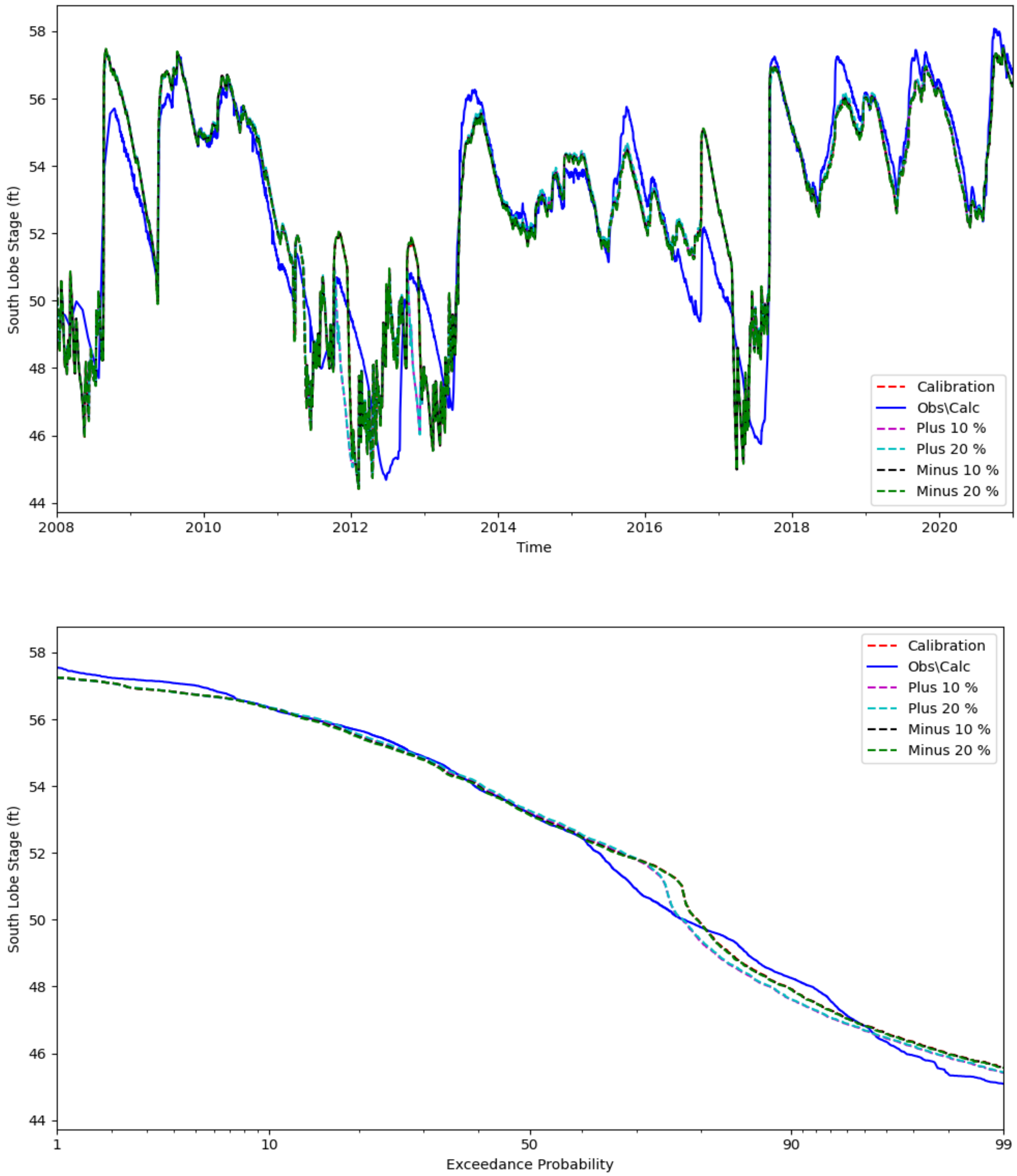

Figure 34. Impact of INFILT on simulated stages of the South Lobe of Lake Prevatt (ft NAVD88)

LONG-TERM SIMULATION

Using the extended rainfall, PET, and UFA stages, we extended the calibrated and validated HSPF model to the period from 1/1/1953 to 12/31/2020. The daily simulated stages adequately represented the temporal evolutions and variations of the long-term observed stage of Lake Prevatt for the North Lobe (Figure 35) and South Lobe (Figure 36). The trends in the hydrographs for both lobes are fairly even over time, with a slight decrease in average stage over time. In the early period of the timeseries, simulated stage was slightly higher with less variability, while in the later period the stage was lower with higher variability. Factors that may contribute to these trends include variability in rainfall, changing conditions on the watershed itself such as land cover changes due to development, and increases in groundwater pumping over time.

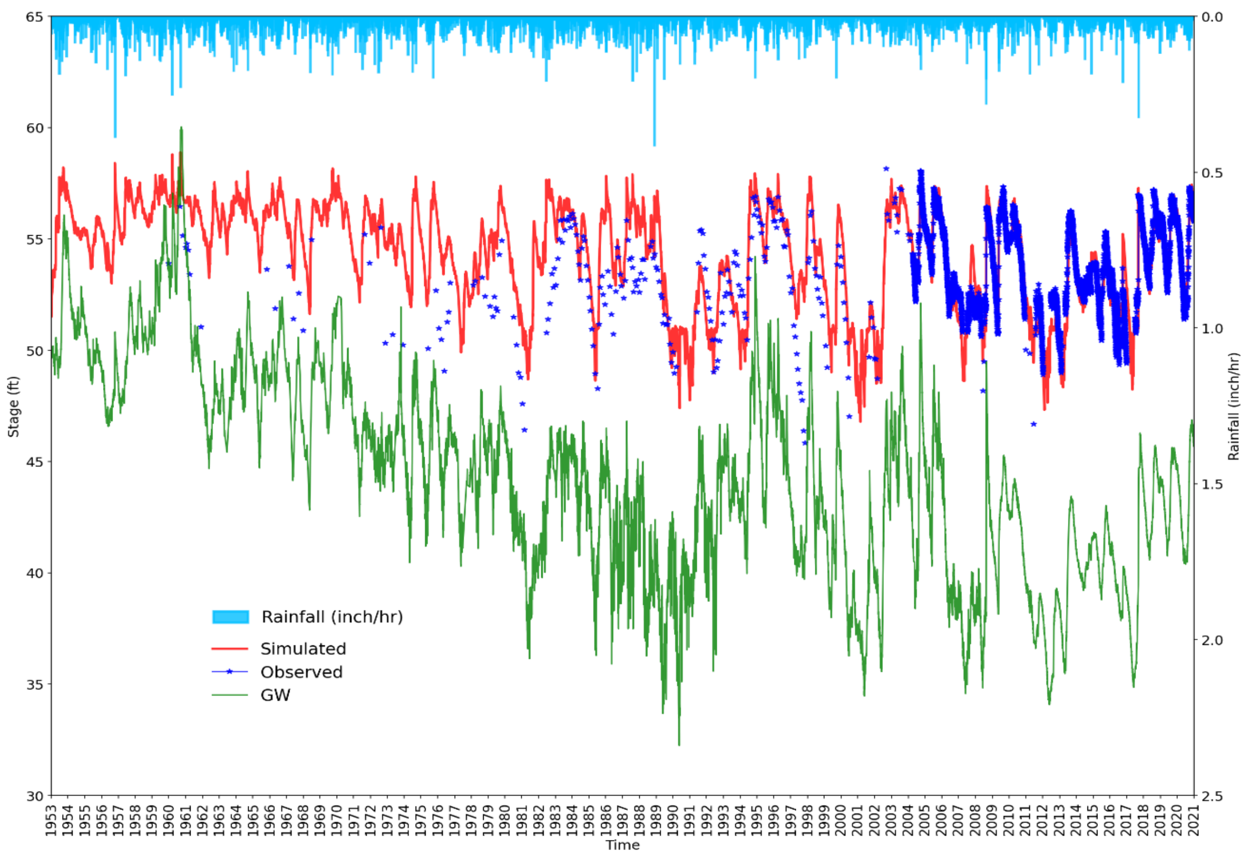

Figure 35. Daily long-term observed and simulated stages of the North Lobe of Lake Prevatt (ft NAVD88)

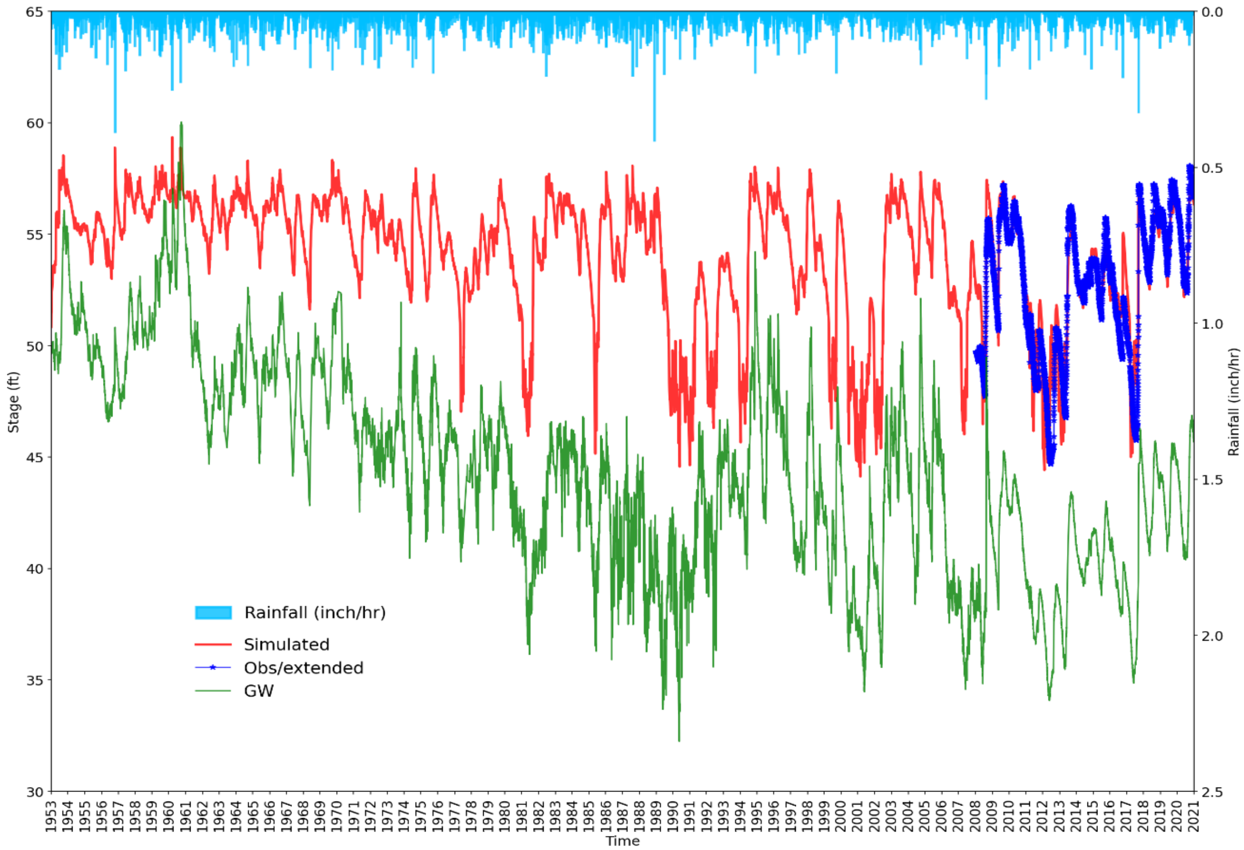

Figure 36. Daily long-term observed and simulated stages of the South Lobe of Lake Prevatt (ft NAVD88)

SUMMARY AND CONCLUSIONS

In support of hydrologic and MFL modeling of Lake Prevatt, we collected, reviewed, and analyzed available hydro-meteorological and geo-spatial data of the Prevatt watershed. Based on the available hydro-meteorological and GIS data, we set up the model for the period 1995 to 2020, calibrated the model for the period 2008 to 2020, and validated it for the period 1995 to 2007. We subsequently extended the calibrated and validated model to the period from 1953 to 2020 for long-term simulations. We also conducted a parameter sensitivity analysis for the calibration period of the extended model and determined the most sensitive parameters for the model.

The HSPF model reasonably reproduced the observed daily water stages for Lake Prevatt for both calibration and validation periods. Most of the daily statistical values met the targeted values, especially the percent of observations bracketed within ± 1ft and Nash-Sutcliffe Efficiency (NSE). The model adequately replicated the long-term daily observed stages of the lake, achieving acceptable statistical evaluation values and performance ratings. We also identified that the leakance and lower zone ET parameters are the most sensitive parameters for modeling the hydrologic processes of Lake Prevatt. Overall, the HSPF model showed reasonable simulations of surface water-groundwater interaction processes and the water budget of Lake Prevatt, indicating the model can be used for MFL modeling and analysis.

REFERENCES

Boniol D. and Mouyard K. (2016). Recharge to the Upper Floridan Aquifer in the St. Johns River Water Management District, Florida. Technical Fact Sheet SJ2016-FS1.

Campolongo F., Saltelli A. and Cariboni J. (2010). From screening to quantitative sensitivity analysis. A unified approach. Computer Physics Communications 182(4): 978-988. https://doi:10.1016/j.cpc.2010.12.039.

Cera, T., Smith, D.S., Cullum, M.G., Adkins, M., Amoah, J., Clapp, D., Freeman, R., Hafner, M., Huang, X., Jia, Y., Jobes, T., and Mao, M. 2012. St. Johns River water supply impact study, chapter 3: watershed hydrology. St. Johns River Water Management District, Palatka, FL.

Fox, S. (2023). DRAFT Appendix F: Lake Prevatt Topobathy DEM Development.

Helsel, D.R. and Hirsch, R.M. (2002). Statistical Methods in Water Resources (Chapter A3). Available at http://pubs.er.usgs.gov/publication/twri04A3.

Jobes, T. (2022). HSPF Common Logic for The St. Johns River Water Management District.

Saltelli, A., Tarantola S., Campolongo. F., and Ratto M. (2004). Sensitivity Analysis in Practice: A Guide to Assessing Scientific Models. John Wiley & Sons.

ATTACHMENT

Attachment - 1. Stage-Area and Stage-Volume dataset for the North Lobe

Stage (ft NAVD88)	North Lobe Area (acres)	North Lobe Volume (ac-ft)
46.2	0.01	0
46.3	0.01	0
46.4	0.01	0
46.5	0.02	0
46.6	0.02	0.01
46.7	0.02	0.01
46.8	0.02	0.01
46.9	0.02	0.01
47	0.02	0.01
47.1	0.04	0.02
47.2	0.05	0.02
47.3	0.07	0.03
47.4	0.1	0.04
47.5	0.14	0.05
47.6	0.2	0.07
47.7	0.28	0.09
47.8	0.37	0.12
47.9	0.48	0.16
48	0.58	0.22
48.1	0.7	0.28
48.2	0.84	0.36
48.3	0.98	0.45
48.4	1.13	0.56
48.5	1.27	0.68
48.6	1.41	0.81
48.7	1.57	0.96
48.8	1.71	1.12
48.9	1.84	1.3
49	1.98	1.49
49.1	2.16	1.7
49.2	2.37	1.92
49.3	2.59	2.17
49.4	2.85	2.44

49.5	3.15	2.74
49.6	3.43	3.07
49.7	3.69	3.43
49.8	3.93	3.81
49.9	4.11	4.21
50	4.27	4.63
50.1	4.44	5.07
50.2	4.62	5.52
50.3	4.82	5.99
50.4	5.03	6.48
50.5	5.25	7
50.6	5.51	7.54
50.7	5.79	8.1
50.8	6.05	8.69
50.9	6.54	9.32
51	7.06	10
51.1	7.62	10.73
51.2	8.18	11.52
51.3	8.57	12.36
51.4	8.89	13.24
51.5	9.16	14.14
51.6	9.43	15.07
51.7	9.74	16.03
51.8	10.05	17.02
51.9	10.31	18.03
52	10.47	19.07
52.1	10.61	20.13
52.2	10.74	21.19
52.3	10.86	22.27
52.4	11	23.37
52.5	11.12	24.47
52.6	11.25	25.59
52.7	11.38	26.72
52.8	11.54	27.87
52.9	11.71	29.03
53	11.84	30.21
53.1	12.06	31.4
53.2	13.1	32.66

53.3	13.84	34.01
53.4	14.68	35.43
53.5	15.49	36.94
53.6	16.94	38.56
53.7	17.67	40.3
53.8	18.09	42.09
53.9	18.41	43.91
54	18.63	45.76
54.1	18.79	47.64
54.2	18.89	49.52
54.3	19.06	51.42
54.4	19.29	53.33
54.5	19.44	55.27
54.6	19.6	57.22
54.7	19.74	59.19
54.8	19.88	61.17
54.9	19.93	63.16
55	19.96	65.16
55.1	19.98	67.16
55.2	20.01	69.15
55.3	20.23	71.16
55.4	21.12	73.23
55.5	22.24	75.39
55.6	23.11	77.66
55.7	23.79	80.01
55.8	24.3	82.42
55.9	24.73	84.87
56	25.09	87.36
56.1	25.42	89.89
56.2	25.74	92.44
56.3	26.04	95.03
56.4	26.33	97.65
56.5	26.6	100.3
56.6	26.88	102.97
56.7	27.15	105.67
56.8	27.46	108.4
56.9	27.79	111.17
57	28.12	113.96

57.1	28.45	116.79
57.2	28.8	119.65
57.3	29.14	122.55
57.4	29.54	125.48
57.5	29.95	128.46
57.6	30.34	131.47
57.7	30.77	134.53
57.8	31.17	137.63
57.9	31.59	140.76
58	31.99	143.94
58.1	32.4	147.16
58.2	32.79	150.42
58.3	33.16	153.72
58.4	33.53	157.05
58.5	33.91	160.43
58.6	34.3	163.84
58.7	34.69	167.29
58.8	35.08	170.78
58.9	35.47	174.3
59	35.87	177.87
59.1	36.24	181.48
59.2	36.59	185.12
59.3	36.93	188.79
59.4	37.24	192.5
59.5	37.52	196.24
59.6	37.76	200
59.7	37.98	203.79
59.8	38.17	207.6
59.9	38.33	211.43
60	38.47	215.27
60.1	38.59	219.12
60.2	38.69	222.98
60.3	38.77	226.86
60.4	38.84	230.74
60.5	38.9	234.62
60.6	38.95	238.52
60.7	38.98	242.41
60.8	39.02	246.31

Attachment - 2. Stage-Area and Stage-Volume dataset for the South Lobe

Stage (ft NAVD88)	South Lobe Area (acres)	South Lobe Volume (ac-ft)
43.2	0	0
43.3	0	0
43.4	0	0
43.5	0	0
43.6	0	0
43.7	0	0
43.8	0	0
43.9	0	0
44	0.01	0
44.1	0.01	0
44.2	0.02	0
44.3	0.02	0.01
44.4	0.03	0.01
44.5	0.04	0.01
44.6	0.05	0.02
44.7	0.06	0.02
44.8	0.06	0.03
44.9	0.08	0.03
45	0.09	0.04
45.1	0.1	0.05
45.2	0.11	0.06
45.3	0.13	0.07
45.4	0.15	0.09
45.5	0.17	0.1
45.6	0.19	0.12
45.7	0.21	0.14
45.8	0.23	0.16
45.9	0.26	0.19
46	0.29	0.22
46.1	0.33	0.25
46.2	0.36	0.28
46.3	0.39	0.32
46.4	0.42	0.36
46.5	0.45	0.4
46.6	0.48	0.45

46.7	0.5	0.5
46.8	0.54	0.55
46.9	0.57	0.61
47	0.62	0.67
47.1	0.74	0.73
47.2	0.81	0.81
47.3	0.89	0.9
47.4	0.98	0.99
47.5	1.13	1.09
47.6	1.42	1.22
47.7	1.69	1.37
47.8	2.03	1.56
47.9	2.39	1.78
48	2.85	2.04
48.1	3.37	2.35
48.2	3.95	2.72
48.3	4.81	3.15
48.4	6.38	3.71
48.5	7.24	4.4
48.6	8.09	5.16
48.7	8.97	6.01
48.8	9.87	6.96
48.9	11.08	8
49	12.51	9.19
49.1	13.52	10.49
49.2	14.12	11.88
49.3	14.48	13.31
49.4	14.81	14.77
49.5	15.14	16.27
49.6	15.48	17.8
49.7	15.87	19.37
49.8	16.29	20.97
49.9	16.76	22.63
50	17.32	24.33
50.1	17.97	26.09
50.2	18.89	27.93
50.3	20.17	29.88
50.4	21.52	31.96

50.5	22.89	34.19
50.6	24.23	36.54
50.7	25.58	39.03
50.8	26.98	41.66
50.9	28.59	44.43
51	30.41	47.39
51.1	32.27	50.52
51.2	34.87	53.87
51.3	38.32	57.52
51.4	41.23	61.5
51.5	44.05	65.77
51.6	46.62	70.31
51.7	49.17	75.11
51.8	50.84	80.11
51.9	52.46	85.27
52	53.42	90.56
52.1	54.17	95.94
52.2	54.86	101.39
52.3	55.63	106.93
52.4	56.1	112.51
52.5	56.54	118.15
52.6	56.97	123.82
52.7	57.38	129.54
52.8	58.18	135.33
52.9	58.94	141.17
53	59.12	147.08
53.1	59.14	152.99
53.2	59.3	158.91
53.3	59.46	164.85
53.4	60.05	170.82
53.5	61.08	176.87
53.6	62.55	183.05
53.7	64.48	189.4
53.8	66.12	195.93
53.9	67.56	202.62
54	68.76	209.44
54.1	69.68	216.36
54.2	70.39	223.37

54.3	70.97	230.43
54.4	71.61	237.56
54.5	72.44	244.76
54.6	73.19	252.05
54.7	73.66	259.39
54.8	74.02	266.78
54.9	74.56	274.2
55	74.74	281.67
55.1	74.91	289.15
55.2	75.04	296.65
55.3	75.46	304.17
55.4	76.65	311.76
55.5	78.4	319.52
55.6	80	327.44
55.7	81.32	335.51
55.8	82.49	343.7
55.9	83.46	352
56	84.33	360.39
56.1	85.16	368.86
56.2	86	377.42
56.3	86.81	386.06
56.4	87.56	394.78
56.5	88.27	403.57
56.6	88.97	412.43
56.7	89.66	421.36
56.8	90.35	430.36
56.9	91.01	439.43
57	91.7	448.57
57.1	92.39	457.77
57.2	93.07	467.05
57.3	93.74	476.39
57.4	94.41	485.79
57.5	95.07	495.27
57.6	95.7	504.81
57.7	96.34	514.41
57.8	96.97	524.07
57.9	97.62	533.8
58	98.25	543.6

58.1	98.88	553.45
58.2	99.48	563.37
58.3	100.1	573.35
58.4	100.71	583.39
58.5	101.32	593.49
58.6	101.94	603.65
58.7	102.54	613.88
58.8	103.12	624.16
58.9	103.71	634.5
59	104.28	644.9
59.1	104.87	655.36
59.2	105.43	665.88
59.3	105.99	676.45
59.4	106.54	687.07
59.5	107.06	697.75
59.6	107.55	708.48
59.7	108.01	719.26
59.8	108.43	730.08
59.9	108.84	740.95
60	109.21	751.85
60.1	109.53	762.79
60.2	109.82	773.76
60.3	110.11	784.75
60.4	110.36	795.78
60.5	110.6	806.82
60.6	110.81	817.9
60.7	111	828.99
60.8	111.18	840.1